

---

# A Unified Solution for Privacy and Communication Efficiency in Vertical Federated Learning (Supplemental Material)

---

Anonymous Author(s)

Affiliation

Address

email

## 1 A Notation Table

2 Below is a notation table for the parameter used in the convergence analysis.

Table 1: Notation Table

Basic:	
$\mathbf{w} = [w_1, w_2, \dots, w_M]$	The parameter for all the clients.
$h_{m,i} = h_m(w_m; x_{m,i})$	The local model output of client $m$ with sample $i$
$\Phi_i = \Phi_i(\mathbf{w}) = [h_1(w_1; x_{1,i}), \dots, h_M(w_M; x_{M,i})] = [h_{1,i}, \dots, h_{M,i}]$	The output embeddings from all clients for sample $i$
$f(w_0, \mathbf{w}) = f(w_0, \mathbf{w}, X, y)$	The global loss function
$f_i(w_0, \Phi_i(\mathbf{w})) = f_i(w_0, h_{1,i}, \dots, h_{M,i})$	The loss function for the sample $i$ calculated by server.
With timestep ( $t$ ), clients' delay ( $\tilde{\mathbf{w}}$ ), embedding compression ( $\hat{f}$ ), ZOO gradient estimator ( $\hat{\nabla}$ )	
$w_m^t$	The client $m$ 's parameter, at global timestep $t$ ,
$\mathbf{w}^t = [w_1^t, \dots, w_M^t]$	The clients' parameter at global timestep $t$
$\tilde{\mathbf{w}}^t = \mathbf{w}^{t-\tau^t} = [w_1^{t-\tau_1^t}, \dots, w_M^{t-\tau_M^t}]$	The delayed parameter for all the clients at global time step $t$ (and the local timestep is 0 for all $w$ ).
$\Phi_i^t = \Phi_i(\mathbf{w}^t) = [h_1(w_1^t; x_{1,i}), \dots, h_M(w_M^t; x_{M,i})]$	The output embeddings from all clients for sample $i$ at global timestep $t$ without delay.
$\tilde{\Phi}_i^t = \Phi_i(\tilde{\mathbf{w}}^t) = [h_1(w_1^{t-\tau_1^t}; x_{1,i}), \dots, h_M(w_M^{t-\tau_M^t}; x_{M,i})]$	The output embeddings from all clients for sample $i$ with the client delay at global timestep $t$
$\Phi_i^t(w_m^t) = [h_1(w_1^t; x_{1,i}), \dots, h_m(w_m^t; x_{m,i}), \dots, h_M(w_M^t; x_{M,i})]$	$\Phi_i^t$ substitute the client $m$ 's parameter with $w_m^t$
$\tilde{\Phi}_i^t(w_m^t) = [h_1(w_1^{t-\tau_1^t}; x_{1,i}), \dots, h_m(w_m^t; x_{m,i}), \dots, h_M(w_M^{t-\tau_M^t}; x_{M,i})]$	$\tilde{\Phi}_i^t$ substitute the client $m$ 's parameter with $w_m^t$
$\hat{f}_i(w_0, \Phi_i) = f_i(w_0, h_{1,i} + \epsilon_{1,i}, \dots, h_{M,i} + \epsilon_{M,i})$	The loss function with compression error of all client's embedding.
$\hat{\nabla}_{h_{m,i}} f_i(w_0, \Phi_i) = \frac{\phi(d_{h_m})}{\mu_m} [f_i(h_{m,i} + \mu_m u_{m,i}) - f_i(h_{m,i})] u_{m,i}$	The ZO gradient estimator w.r.t. the client $m$ 's output

---

### 3 B Assumptions

4 Assumptions B.1 - B.4 are the basic assumptions for solving the non-convex optimization problem  
5 with stochastic gradient descent [10, 15, 21].

6 **Assumption B.1. Feasible Optimal Solution:** Function  $f$  is bounded below that is, there exist  $f^*$   
7 such that,

$$f^* := \inf_{[w_0, \mathbf{w}] \in \mathbb{R}^d} f(w_0, \mathbf{w}) > -\infty.$$

8 **Assumption B.2. Lipschitz Gradient:**  $\nabla f_i$  is  $L$ -Lipschitz continuous w.r.t. all the parameter, i.e.,  
9 there exists a constant  $L$  for  $\forall [w_0, \mathbf{w}], [w'_0, \mathbf{w}']$  such that

$$\|\nabla_{[w_0, \mathbf{w}]} f_i(w_0, \Phi_i(\mathbf{w})) - \nabla_{[w'_0, \mathbf{w}']} f_i(w'_0, \Phi_i(\mathbf{w}'))\| \leq L \|[w_0, \mathbf{w}] - [w'_0, \mathbf{w}']\|$$

10 specifically there exists an  $L_m > 0$  for all parties  $m = 0, \dots, M$  such that  $\nabla_{w_m} f_i$  is  $L_m$ -Lipschitz  
11 continuous:

$$\|\nabla_{w_m} f_i(w_0, \Phi_i(\mathbf{w})) - \nabla_{w_m} f_i(w'_0, \Phi_i(\mathbf{w}'))\| \leq L_m \|[w_0, \mathbf{w}] - [w'_0, \mathbf{w}']\|$$

12 **Assumption B.3. Unbiased Gradient:** For  $m \in 0, 1, \dots, M$  for every data sample  $i$ , the stochastic  
13 partial derivatives are unbiased, i.e.  $\mathbb{E}_i \nabla_{w_m} f_i(w_0, \Phi_i(\mathbf{w})) = \nabla_{w_m} f(w_0, \Phi_i(\mathbf{w}))$

14 **Assumption B.4. Bounded Variance:** For  $m = 0, 1, \dots, M$ , there exist constants  
15  $\sigma_m \leq \infty$  such that the variance of the stochastic partial derivatives are bounded:  
16  $\mathbb{E}_i \|\nabla_{w_m} f_i(w_0, \Phi_i(\mathbf{w})) - \nabla_{w_m} f(w_0, \mathbf{w})\|^2 \leq \sigma_m^2$

17 Assumptions B.5 - B.6 are the base assumptions for bounding the compression of the embedding  
18 on the loss [4]. Since compression introduces error in the input of the loss function, therefore with  
19 the bounded Hessian we can derive the maximum effect of the error on the loss. And bounding the  
20 block-coordinated gradient is common in VFL analysis for bounding the gradient for the entire model  
21 when the gradient of other parts have been bounded [4, 12, 22].

22 **Assumption B.5. Bounded Hessian:** The Hessian for  $f_i(w_0, \Phi_i(\mathbf{w}))$  is bounded, i.e. there exist  
23 positive constant  $H_m$  for  $m = 0, 1, \dots, M$  such that for all  $[w_0, \mathbf{w}]$ , the following inequalities holds:

$$\begin{aligned} \|\nabla_{w_0}^2 f_i(w_0, \Phi_i(\mathbf{w}))\| &\leq H_0 \\ \|\nabla_{(w_m; x_{m,i})}^2 f_i(w_0, \Phi_i(\mathbf{w}))\| &\leq H_m \end{aligned}$$

24 Where the norm is the spectral norm (the matrix norm induced by L2-norm<sup>1</sup>)

25 **Assumption B.6. Bounded Block-coordinate Gradient:** The gradient of all the participants' local  
26 output w.r.t. their local input is bounded, i.e. there exist positive constants  $\mathbf{G}_0$  for the server  $m = 0$   
27 the following inequalities holds:

$$\|\nabla_{[w_0, h_{1,i}, \dots, h_{M,i}]} f_i(w_0, h_{1,i}, \dots, h_{M,i})\| \leq \mathbf{G}_0$$

28 and there exist positive constants  $\mathbf{G}_m$  for the client  $m = 1, \dots, M$  the following inequalities hold:

$$\|\nabla_{w_m}(w_m; x_{m,i})\| \leq \mathbf{G}_m$$

29 where the first inequality bounds the gradient for the server w.r.t. to all the outputs received from the  
30 clients, and the second inequality bounds the gradient for the client's outputs w.r.t. the client's local  
31 parameter.

32 Assumptions B.7 - B.8 are the assumptions for dealing with the asynchronous updates of our VFL  
33 framework. We assume that the activation of clients at each global round is independent and that the  
34 maximum delay is bounded [21, 5, 12]. These are reasonable assumptions for analysis.

35 **Assumption B.7. Independent Client:** The activated client  $m_t$  for the global iteration  $t$  is indepen-  
36 dent of  $m_0, \dots, m_{t-1}$  and satisfies  $\mathbb{P}(m_t = m) := p_m$

37 **Assumption B.8. Uniformly Bounded Delay:** For each client  $m$ , and each sample  $i$ , the delay at  
38 each global iteration  $t$  is bounded by a constant  $\tau$ . i.e.  $\tau_{m,i}^t \leq \tau$

<sup>1</sup>For notation brevity, unless specific, the norm is L2-norm for the vector and spectral norm for the matrix.

## 39 C Security Analysis

### 40 C.1 Differential Privacy Guarantee of Sharing the Stochastic Estimation of the Gradient

41 **Definition C.1.**  $(\epsilon, \delta)$ -**Differential Privacy** A randomized mechanism  $\mathcal{M} : \mathcal{D} \rightarrow \mathcal{R}$  with domain  
42  $\mathcal{D}$  and range  $\mathcal{R}$  satisfies  $(\epsilon, \delta)$ -differential privacy if for any two adjacent inputs  $d, d' \in \mathcal{D}$ , and for  
43 any subset of outputs  $S \subseteq \mathcal{R}$  it holds that:

$$\Pr[\mathcal{M}(d) \in S] \leq e^\epsilon \Pr[\mathcal{M}(d') \in S] + \delta$$

44 Now we start the proof of the  $(\epsilon, \delta)$ -Differential Privacy of the training process of sharing the  
45 stochastic gradient.

46 The activated client  $m_t$  at iteration  $t$  is updated with the following equation.

$$w_{m_t}^{t+1} = w_{m_t}^t - \eta \hat{\nabla}_{h_{m_t,i}} f_i(w_0^t, \Phi_i) \cdot \nabla_{m_t} h_{m_t,i} \quad (1)$$

47 where

$$\hat{\nabla}_{h_{m_t,i}} f_i(w_0^t, \Phi_i) = \frac{1}{q} \sum_{j=1}^q \frac{1}{\mu_{m_t}} [f_i(h_{m_t,i} + \mu_{m_t} \mathbf{u}_{m_t,i}^j) - f_i(h_{m_t,i})] \mathbf{u}_{m_t,i}^j \quad (2)$$

48 For notation brevity, we define:

$$g_{m_t}^{t,j} \triangleq \frac{1}{\mu_{m_t}} [f_i(h_{m_t,i} + \mu_{m_t} \mathbf{u}_{m_t,i}^j) - f_i(h_{m_t,i})] \mathbf{u}_{m_t,i}^j \quad (3)$$

$$g_{m_t}^t \triangleq \hat{\nabla}_{h_{m_t,i}} f_i(w_0^t, \Phi_i) = \frac{1}{q} \sum_{j=1}^q g_{m_t}^{t,j} \quad (4)$$

49 We will show in the following lemma C.2 that the solution can be regarded as client updating with the  
50 unbiased gradient of the smoothed loss function  $f_{\mathbf{u},i}(w_0^t, \Phi_i) = \mathbb{E}_{\mathbf{u}}[f_i(w_0, \Phi(\mathbf{w})) + \mu \mathbf{u}]$ , but adding  
51 a stochastic noise on it, where the unbiased ideal parameter sequence of the client  $m_t$  is defined as  
52  $\check{w}_{m_t}$ . Formally:

$$\check{w}_{m_t}^{t+1} = \check{w}_{m_t}^t - \eta \nabla_{h_{m_t,i}} f_{\mathbf{u},i}(w_0^t, \Phi_i) \cdot \nabla_{m_t} h_{m_t,i} \quad (5)$$

$$w_{m_t}^t = \check{w}_{m_t}^t + \xi_{m_t}^t \quad (6)$$

53 Where  $\xi^t$  is a stochastic variable.

54 For notation brevity, we define:

$$\check{g}_{m_t}^t \triangleq \nabla_{h_{m_t,i}} f_{\mathbf{u},i}(w_0^t, \Phi_i) \quad (7)$$

55 **Lemma C.2.** For  $t = 0, \dots, T-1$ , if  $g_{m_t}^{t,j}$  is i.i.d. and  $q$  is sufficiently large, then  $w_{m_t}^t$  is distributed as:

$$w_{m_t}^t \sim \mathcal{N}\left(\check{w}_{m_t}^t, \frac{1}{q} \eta^2 (\nabla_{m_t} h_{m_t,i})^\top \Psi_{m_t}^t \nabla_{m_t} h_{m_t,i}\right) \quad (8)$$

56 and  $g_{m_t}^t$  is distributed as

$$g_{m_t}^t \sim \mathcal{N}\left(\check{g}_{m_t}^t, \frac{1}{q} \Psi_{m_t}^t\right) \quad (9)$$

57 *proof:* First we show that  $\mathbb{E}[w_{m_t}^t] = \check{w}_{m_t}^t$ , we prove this by Mathematical Induction. The  $w_{m_t}^0 = \check{w}_{m_t}^0$   
58 holds by natural when initializing the parameter. Assuming  $\mathbb{E}[w_{m_t}^{t-1}] = \check{w}_{m_t}^{t-1}$ , we have:

$$\begin{aligned} \mathbb{E}[w_{m_t}^t] &= \mathbb{E}[w_{m_t}^{t-1} - \eta \hat{\nabla}_{h_{m_t,i}} f_i(w_0^t, \Phi_i) \cdot \nabla_{m_t} h_{m_t,i}^t] \\ &= \check{w}_{m_t}^{t-1} - \eta \mathbb{E}[\hat{\nabla}_{h_{m_t,i}} f_i(w_0^t, \Phi_i) \cdot \nabla_{m_t} h_{m_t,i}^t] \end{aligned}$$

$$\begin{aligned}
&= \check{w}_{m_t}^{t-1} - \eta \nabla_{h_{m_t,i}} f_{\mathbf{u},i}(w_0^t, \Phi_i) \cdot \nabla_{m_t} h_{m_t,i}^t \\
&= \check{w}_{m_t}^t
\end{aligned} \tag{10}$$

59 Where the third equality applies the lemma D.3 (Eq. 26). Therefore  $\mathbb{E}[w_{m_t}^t] = \check{w}_{m_t}^t$  for  $t =$   
60  $0, 1, \dots, T-1$ .

61 For the stochastic gradient estimation  $g_{m_t}^t$  which applies  $q$  times of sampling on the same distribution  
62 centering on  $w_{m_t}^t$ . Apply the central limit theorem, and assuming the expectation and covariance  
63 matrix for each sampling is  $\mu_{m_t}^t$  and  $\Psi_{m_t}^t$  respectively, we have

$$g_{m_t}^t = \frac{1}{q} \sum_{j=1}^q g_{m_t}^{t,j} \sim \mathcal{N}(\mu_{m_t}^t, \frac{1}{q} \Psi_{m_t}^t) \tag{11}$$

64 The update of the  $w_{m_t}^t$  is distributed as:

$$-\eta g_{m_t}^t \nabla_{m_t} h_{m_t,i} \sim \mathcal{N}\left(-\eta \mu_{m_t}^t \nabla_{m_t} h_{m_t,i}, \frac{1}{q} \eta^2 (\nabla_{m_t} h_{m_t,i})^\top \Psi_{m_t}^t \nabla_{m_t} h_{m_t,i}\right) \tag{12}$$

65 which is the only stochastic part, therefore we have

$$w_{m_t}^t \sim \mathcal{N}\left(\check{w}_{m_t}^t, \frac{1}{q} \eta^2 (\nabla_{m_t} h_{m_t,i})^\top \Psi_{m_t}^t \nabla_{m_t} h_{m_t,i}\right) \tag{13}$$

66 the first part of the lemma has been proved.

67 Specifically,  $\mathbb{E}[g_{m_t}^t] = \check{g}_{m_t}^t$  (lemma D.3 Eq. 26), therefore we have

$$g_{m_t}^t = \frac{1}{q} \sum_{j=1}^q g_{m_t}^{t,j} \sim \mathcal{N}\left(\check{g}_{m_t}^t, \frac{1}{q} \Psi_{m_t}^t\right) \tag{14}$$

68 the second part of the lemma has been proved.  $\square$

69 **Lemma C.3.**  $(\epsilon, \delta)$ -Differential Privacy for Gaussian mechanism: Let  $\epsilon \in (0, 1)$  be arbitrary, for  
70  $c^2 > 2 \ln(1.25/\delta)$  the Gaussian mechanism with parameter  $\sigma > c \Delta_2 / \epsilon$  is  $(\epsilon, \delta)$ -differential privacy.

71 *proof:* The proof is in [6] Theorem A.1.

72 **Theorem C.4.** Let  $\epsilon \in [0, 1]$ , the covariance matrix of the  $g_{m_t}^t$  be  $\Psi_{m_t}^t$ , with the following condition  
73 holds:

$$\sigma_{m_t,s} = \sqrt{\frac{1}{qd_h T} \sum_{t=0}^{T-1} \text{tr}(\Psi_{m_t}^t)} > \frac{2\sqrt{2 \ln(1.25/\delta)} \mathbf{G}_0}{N \cdot \epsilon} \tag{15}$$

74 under Algorithm 1, sharing the stochastic estimation of the partial gradient for each iteration satisfy  
75  $(\epsilon, \delta)$ -differential privacy.

76 *Proof:* From lemma C.2 we already have that:

$$g_{m_t}^t \sim \mathcal{N}\left(\check{g}_{m_t}^t, \frac{1}{q} \Psi_{m_t}^t\right) \tag{16}$$

77 To make the problem more trackable, assume each entry of  $g_{m_t}^t$  is independent of each other and has  
78 the same variance value, and the variance is stable throughout the training process. Therefore, for  
79 each entry  $s$  of  $g_{m_t}^t$

$$g_{m_t,s}^t \sim \mathcal{N}(\check{g}_{m_t,s}^t, \sigma_{m_t,s}^t) \tag{17}$$

80 where  $\sigma_{m_t} = \frac{1}{qd_h T} \sum_{t=0}^{T-1} \text{tr}(\Psi_{m_t}^t)$  is the averaged variance for each entry.

81 The  $l_2$ -norm sensitive of  $g_{m_t}^t$  is given by

$$\Delta_{m_t,2} = \max_{\mathcal{D}, \mathcal{D}'} \|\check{g}_{m_t, \mathcal{D}}^t - \check{g}_{m_t, \mathcal{D}'}^t\|_2 \tag{18}$$

82 Assume the probability of selecting each sample in the dataset  $\mathcal{D}$  (or  $\mathcal{D}'$ ) is the same.  $\mathcal{D}$  and  $\mathcal{D}'$  are  
 83 two neighboring dataset differing in only one sample  $(x_i, y_i)$  and  $(x'_i, y'_i)$ . Without loss of generality,  
 84 we set the differing sample to be the  $N$ -th sample. Assume  $\zeta = \max_{m_t, i} \|\nabla_{h_{m_t, i}} f_{\mathbf{u}, i}(w_0^t, \Phi_i)\|$  be  
 85 the maximum  $l_2$ -norm of the partial gradient w.r.t. any client's output through the entire training.

$$\begin{aligned}
 \Delta_{m_t, 2} &= \max_{\mathcal{D}, \mathcal{D}'} \left\| \frac{1}{N} \sum_{i=0}^N \nabla_{h_{m_t, i}} f_{\mathbf{u}, i}(w_0^t, \Phi_i) - \frac{1}{N} \sum_{i=0}^{N-1} \nabla_{h_{m_t, i}} f_{\mathbf{u}, i}(w_0^t, \Phi_i) \right. \\
 &\quad \left. - \frac{1}{N} \nabla_{h_{m_t, N}} f_{\mathbf{u}, N}(w_0^t, h_1(w_1; x'_{1, N}), h_2(w_2; x'_{2, N}); y'_N) \right\|_2 \\
 &= \frac{1}{N} \max_{\mathcal{D}, \mathcal{D}'} \left\| [\nabla_{h_{m_t, i}} f_{\mathbf{u}, i}(w_0^t, \Phi_i) - \nabla_{h_{m_t, N}} f_{\mathbf{u}, N}(w_0^t, h_1(w_1; x'_{1, N}), h_2(w_2; x'_{2, N}); y'_N)] \right\|_2 \\
 &\leq \frac{2\zeta}{N} \tag{19}
 \end{aligned}$$

86 where the inequality is based on assumption B.6.

87 Applying lemma C.3, with the  $l_2$ -norm sensitive  $\Delta_{m_t, 2}$  of  $\check{g}_m$ . We derived the Theorem C.4.  $\blacksquare$

88 **Total Privacy** Now we consider the total privacy of the entire training process.

89 **Lemma C.5. (Advanced Composition)** For all  $\epsilon, \delta, \delta'$  the class of  $(\epsilon, \delta)$ -DP mechanisms satisfies  
 90  $(\epsilon', k\delta + \delta')$ -DP under  $k$ -fold adaptive composition for:

$$\epsilon' = \sqrt{2k \ln(1/\delta')} \epsilon + k\epsilon(e^\epsilon - 1) \tag{20}$$

91 *Proof:* The proof is from [6, Theorem 3.20].

92 **Theorem C.6.** Under the “honest-but-colluded” threat model where the attacker can access all  
 93 information of all clients through the entire training process. Under algorithm 1, if the following  
 94 condition holds:

$$\frac{1}{qd_h T} \sum_{t=0}^{T-1} \eta \text{tr}(\Psi_{m_t}^t) > \frac{2\zeta \sqrt{2 \ln(1.25/\delta)}}{N \cdot \epsilon} \tag{21}$$

95 we can derive that sharing the stochastic gradient estimation from the server ensures  $(\epsilon', T\delta + \delta')$ -DP  
 96 for all  $\epsilon, \delta, \delta' > 0$ , where  $\epsilon' = \sqrt{2T \ln(1/\delta')} \epsilon + T\epsilon(e^\epsilon - 1)$ .

97 *Proof:* Theorem C.4 has proved the  $(\epsilon, \delta)$ -DP for each iteration, then applying lemma C.5 with the  
 98 number of composition  $k = T$ , the theorem is proved.  $\blacksquare$

99 **Lemma C.7.** Given target privacy parameters  $0 < \epsilon' < 1$  and  $\delta' > 0$ , to ensure  $(\epsilon', k\delta + \delta')$   
 100 cumulative privacy loss over  $k$  mechanisms, it suffices that each mechanism is  $(\epsilon, \delta)$ -differentially  
 101 private, where

$$\epsilon = \epsilon' / (2\sqrt{2k \ln(1/\delta')}) \tag{22}$$

102 *Proof:* The proof is from [6, Corollary 3.21]

103 **Corollary C.8.** With algorithm 1, for each iteration, for all  $\delta > 0$ , if the following conditions holds:

$$\frac{1}{qd_h T} \sum_{t=0}^{T-1} \eta \text{tr}(\Psi_{m_t}^t) > \frac{4\zeta \sqrt{4T \ln(1.25/\delta) \cdot \ln(1/\delta')}}{N \cdot \epsilon'} \tag{23}$$

104 we can derived  $(\epsilon', T\delta + \delta')$  cumulative privacy loss over  $T$  iteration,

105 *Proof:* Applying lemma C.7 and plugging in  $\epsilon = \epsilon' / (2\sqrt{2T \ln(1/\delta')})$

## 106 C.2 Defense Against the State-of-the-art Privacy Inference Attack in VFL

107 **Privacy Protection of VFL-CZOFO at Framework Level** VFL-CZOFO ensures the protection  
108 of *labels* on the server through two key mechanisms. Firstly, the information shared by the server  
109 with the clients is the ZO gradient with intrinsic DP rather than the vulnerable unbiased gradient.  
110 Secondly, the internal details of the server’s model and the domain information associated with the  
111 labels are not disclosed to the client. Thus, the server appears as a black box to the client, allowing  
112 queries from the clients, but responds with noisy outputs to protect privacy.

113 VFL-CZOFO ensures the protection of the *features* on the clients by keeping the internal model  
114 information of the clients not disclosed to the server. Additionally, clients have the flexibility to  
115 utilize any model, which makes them appear as black-box models to the server. As a result, the server  
116 can only obtain the outputs from the black box (client) but does not have access to the corresponding  
117 inputs nor the ability to make adaptive queries.

118 **SOTA Inference Attack under “Honest-but-curious”** We discuss two types of privacy inference  
119 attacks: the label inference attack and the feature inference attack.

120 A label inference attack [8, 17] under the “honest-but-curious” model involves a curious client  
121 attempting to infer the label of the dataset from the server. The “direct label inference” attack  
122 proposed by Fu et al. [8] cannot successfully attack our framework because it relies on a strong  
123 assumption that the client explicitly knows that the server simply sums the output from all clients.  
124 This allows the gradient replied by the server to directly reveal the label information by the sign of  
125 the entries. However, in our framework, we assume that the server can use any model and that the  
126 client does not have access to the server’s model. Additionally, the gradient is not sent to the client in  
127 our framework. The “model completion” attack by Fu et al. [8] and the “forward embeddings” attack  
128 by Sun et al. [17] rely on the local model’s representation of the unknown label, assuming that the  
129 curious client can obtain a small number of labels for the samples. Essentially, this is equivalent to  
130 using the local model and the local feature set to guess the label. The effectiveness of these attacks  
131 depends solely on the representation of the local model and features held by the client. However,  
132 with Theorem 3, we have proven the  $(\epsilon, \delta)$ -differential privacy of sharing the ZO gradient. Therefore,  
133 the client cannot differ one item from the server’s dataset. Deep Leakage from Gradient and its  
134 variation [24, 23, 13], utilizes gradient information to optimize and reconstruct the label from the  
135 model. However, this attack does not apply to our framework. The attack assumes that the attacker  
136 has access to the target model’s structure and parameters, as well as unbiased gradient information.  
137 In contrast, in our framework, participants cannot access each other’s model information through the  
138 protocol. Additionally, our framework does not provide the attacker with any gradient information.  
139 Instead, the attacker can only obtain a stochastic estimation of the gradient of the ZOO.

140 The feature inference attack [24, 13, 7], involves the server, acting as the attacker, attempting to infer  
141 the feature from the clients under the “honest-but-curious” model. Deep leakage from gradient [24]  
142 can also be used as a feature inference attack in VFL, however, this attack cannot compromise our  
143 framework because the attacker cannot access the victim model and cannot get a certain gradient  
144 information. Model inversions attack [7] can be considered as a feature inference attack, wherein the  
145 server uses the output of the client to recover the feature. However, this attack cannot successfully  
146 compromise our framework because it relies on the attacker adaptively querying the model of the  
147 victim with specially designed input features, which is not allowed in our framework. Specifically,  
148 our framework does not provide a mechanism for the server to query the client with feature inputs.  
149 Moreover, all of the attacks mentioned above assume that the attacker obtained the domain of the  
150 label or features, however, in our framework, the client and server can collaborate without sharing the  
151 tasks information.

152 **“Honest-but-colluded”** In the “honest-but-colluded” threat model, the label inference attack  
153 involves some clients colluding to infer the label from the server [8, 24]. In the worst-case scenario,  
154 all clients collude to infer the label from the server. If there is only one client, the “Honest-but-curious”  
155 threat model is equivalent to the “honest-but-colluded” model since there are no other participants  
156 to collude with. Even in the worst-case scenario where all clients collude, our framework remains  
157 resilient to the “direct label inference” attack described in Fu et al. [8]. This is because the server’s  
158 model remains unknown to the clients, and the clients can only obtain a stochastic estimation of  
159 the gradient, rather than the unbiased gradient information, which makes it impossible for them to  
160 perform the attack successfully. Our framework remains resistant to the Deep Leakage from Gradient

161 attack [24] because this attack relies on the attacker having knowledge of the parameter and structure  
 162 of the victim’s model, which is not shared in our framework. Furthermore, the attacker is unable  
 163 to access the unbiased gradient in our framework, which further prevents this attack from being  
 164 successful.

165 The feature inference attack in the “honest-but-colluded” threat model is that the server colluded with  
 166 some clients to infer the features from one client. In the worst-case scenario, the server colludes with  
 167 all clients except the victim client. The attacker can access all the information from the colluding  
 168 participants, including the model information, the dataset, and the communications between other  
 169 participants, following the protocol. Luo et al. [16] propose a feature inference attack in VFL where  
 170 they assume that all participants collude except the victim client. Additionally, they explicitly assume  
 171 that all clients use the Logistic Regression (LR) model. However, this attack is not applicable to our  
 172 framework because we do not assume a specific model for the client, and the attacker cannot access  
 173 the model information of the victim, making the attack infeasible. The Reverse Multiplication Attack  
 174 [19] is similar to the feature inference attack proposed by Luo et al. [16], but the target model adds  
 175 Homomorphic Encryption to protect the data. In the attack, the authors assume that the “coordinate  
 176 participant” who has the private key is also corrupted, enabling them to decrypt all data received from  
 177 the victim. They then perform an equation-solving attack for the LR model. However, this attack is  
 178 not applicable to our framework because we do not assume an LR model, and the attacker cannot  
 179 access the victim’s model. Therefore, our framework is secure against such attacks.

## 180 D Convergence Analysis

### 181 D.1 Asynchronous VFL Framework

182 We use an Asyn-VFL framework [5] where the server passively handles the request from the clients  
 183 and replies with the necessary information instead of actively sending messages to coordinate with  
 184 the training process of the clients. Asyn-VFL can be modeled with a global iteration sequence, where  
 185 each iteration has four steps. As shown in Fig. 1, step 1 is that the client  $m_t$  is activated and sends the  
 186 forward message to the server. In step 2, the server replies with the necessary information for the  
 187 client’s update. Then the server does local updates based on the updated forward message and the  
 188 client update its model with the backward message.

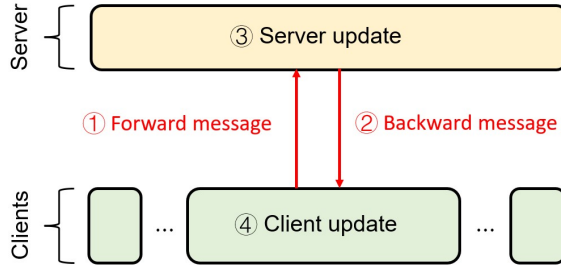


Figure 1: Asynchronous VFL framework

189 At any iteration  $t$ , only one client  $m_t$  and the server updates its parameter. Therefore, there are  
 190 delays between parameters updated at iteration  $t$  and parameters that are not updated. In this paper,  
 191 we use  $\tau_{m,i}^t$  to denote the delay w.r.t. the client  $m$  and the sample  $i$  at global iteration  $t$ . At each  
 192 global iteration, the client  $m_t$  is activated and its delay is clear; for all other clients  $m \neq m_t$ , their  
 193 delay count  $\tau_{m,i}^t$  is increased by 1. Formally, the update rules for delay  $\tau_{m,i}^t$  can be represented as  
 194 following:

$$\tau_{m,i}^{t+1} = \begin{cases} 1, & m = m_t, i = i_t \\ \tau_{m,i}^t + 1, & \text{otherwise} \end{cases}$$

### 195 D.2 Defining Compression Errors

196 **Definition D.1. Compression Error (forward message).** Let vector  $\epsilon_{m,i}$  be the compression error  
 197 of  $\mathcal{C}_m(\cdot)$ , on sample  $i$ , i.e.  $\epsilon_{m,i} = \mathcal{C}_m(h_m(w_m; x_i)) - h_m(w_m; x_i)$ . We denote the expected norm

198 of the error from the client  $m$  at global iteration  $t$  as  $\mathcal{E}_m^t = \mathbb{E} \|\epsilon_{m_t, i_t}\|^2$ , and define the upper limit  
 199  $\mathcal{E} = \max_t \{\mathcal{E}^t\}$

200 **Definition D.2. Compression Error (backward message).** Let  $e_{m,i}$  be the compression error on  
 201  $\delta_{m,i}$ , i.e.  $e_{m,i} = \mathcal{C}_0(\delta_{m,i}) - \delta_{m,i}$ . the pseudo partial derivative that the client gets is

$$\begin{aligned} v_m &= \frac{\phi(d_{h_m})}{\mu_m} [f_i(h_{m,i} + \mu_m \mathbf{u}_{m,i}) - f_i(h_{m,i}) + e_{m,i}] \mathbf{u}_{m,i} \\ &= \frac{\phi(d_{h_m})}{\mu_m} [f_i(h_{m,i} + \mu_m \mathbf{u}_{m,i}) - f_i(h_{m,i})] \mathbf{u}_{m,i} + \frac{\phi(d_{h_m})}{\mu_m} e_{m,i} \mathbf{u}_{m,i} \\ &= \hat{\nabla}_{h_{m,i}} f_i(w_0, \phi_i(\mathbf{w})) + \frac{\phi(d_{h_m})}{\mu_m} e_{m,i} \mathbf{u}_{m,i} \end{aligned} \quad (24)$$

202 Define vector  $\gamma_{m,i} = \frac{\phi(d_{h_m})}{\mu_m} e_{m,i} \mathbf{u}_{m,i}$  be the compression error on  $\hat{\nabla}_{h_{m,i}} f_i(w_0, \phi_i(\mathbf{w}))$ , so that

$$v_m = \hat{\nabla}_{h_{m,i}} f_i(w_0, \phi_i(\mathbf{w})) + \gamma_{m,i} \quad (25)$$

203 and define  $\gamma^t = \gamma_{m_t, i_t}$ , be the error on the activated client  $m_t$  and the selected sample  $i_t$  at iteration  
 204  $T$ , and  $\Gamma^t = \mathbb{E} \|\gamma^t\|^2$ . The upper limit for the compression error is  $\Gamma = \max_t \{\Gamma^t\}$ .

### 205 D.3 Lemmas

206 **Lemma D.3. Zeroth-Order Optimization.** For arbitrary  $f \in C_L^1(\mathbb{R}^d)$ , we have:

207 1)  $f_\mu(x)$  is continuously differentiable, its gradient is Lipschitz continuous with  $L_\mu \leq L$ :

$$\nabla f_\mu(x) = \mathbb{E}_{\mathbf{u}} [\hat{\nabla} f(x)] \quad (26)$$

208 where  $\mathbf{u}$  is drawn from the uniform distribution over the unit Euclidean sphere, and  $\hat{\nabla} f(x) =$   
 209  $\frac{d}{d\mu} [f(x + \mu \mathbf{u}) - f(x)] \mathbf{u}$  is the gradient estimator,  $f_\mu(x) = \mathbb{E}_{\mathbf{u}} [f(x + \mu \mathbf{u})]$  is the smooth approxi-  
 210 mation of  $f$ .

211 2) For any  $x \in \mathbb{R}^d$ ,

$$|f_\mu(x) - f(x)| \leq \frac{L\mu^2}{2} \quad (27)$$

$$\|\nabla f_\mu(x) - \nabla f(x)\|^2 \leq \frac{\mu^2 L^2 d^2}{4} \quad (28)$$

$$\frac{1}{2} \|\nabla f(x)\|^2 - \frac{\mu^2 L^2 d^2}{4} \leq \|\nabla f_\mu(x)\|^2 \leq 2 \|\nabla f(x)\|^2 + \frac{\mu^2 L^2 d^2}{2} \quad (29)$$

212 3) For any  $x \in \mathbb{R}^d$ ,

$$\mathbb{E}_{\mathbf{u}} \left[ \left\| \hat{\nabla} f(x) \right\|^2 \right] \leq 2d \|\nabla f(x)\|^2 + \frac{\mu^2 L^2 d^2}{2} \quad (30)$$

213 Lemma D.3 helps build a connection between  $f(\cdot)$  and its smooth approximation  $f_{\mu_m}(\cdot)$  of the  
 214 convergence analysis. Proof of this lemma is provided in [14, 9].

215 **Lemma D.4. Compression Error.** Under assumption B.5 - B.6, the norm of the difference between  
 216 the loss function value with and without compression error is bounded:

$$\begin{aligned} \mathbb{E} \left\| \nabla_{w_0} \hat{f}_i(w_0^t, \Phi_i^t) - \nabla_{w_0} f_i(w_0^t, \Phi_i^t) \right\|^2 &\leq H_0^2 \mathcal{E} \\ \mathbb{E} \left\| \nabla_{w_m} \hat{f}_i(w_0^t, \Phi_i^t) - \nabla_{w_m} f_i(w_0^t, \Phi_i^t) \right\|^2 &\leq \mathbf{G}_m^2 H_m^2 \mathcal{E} \end{aligned} \quad (31)$$

217 where  $\mathcal{E} = \max_t \{\mathcal{E}^t\} = \max_t \left\{ \sum_{m=1}^M \mathcal{E}_m^t \right\}$

218 *proof:*



219 For notation brevity, we denote:

$$\begin{aligned}
h_{m,i}^t &= h_m(w_m^t; x_{m,i}) \\
\hat{f}_i^t &= f_i(w_0^t, c_{1,i}^t, \dots, c_{q,i}^t) = f_i(w_0, h_{1,i}^t + \epsilon_{1,i}^t, \dots, h_{M,i}^t + \epsilon_{M,i}^t) \\
f_i^t &= f_i(w_0^t, h_{1,i}^t, \dots, h_{M,i}^t) = f_i(w_0^t, \Phi_i^t) \\
E_m^t &= [\epsilon_0^t, \epsilon_1^t, \dots, \epsilon_M^t]
\end{aligned} \tag{32}$$

220 Applying the chain rule to  $\nabla f_i$  w.r.t.  $w_m$ .

$$\begin{aligned}
\nabla_{w_m} \hat{f}_i^t &= \nabla_{w_m} h_{m,i}^t \underbrace{\nabla_{h_{m,i}^t} \hat{f}_i^t}_a \\
&= \nabla_{w_m} h_{m,i}^t \left( \nabla_{h_{m,i}^t} f_i^t + R_0^t \right) \\
&= \nabla_{w_m} f_i^t + \nabla_{w_m} h_{m,i}^t \cdot R_0^t
\end{aligned} \tag{33}$$

221 where a) applies Taylor expansion to  $\nabla_{h_{m,i}^t} \hat{f}_i^t$  around the point  $[w_0^t, \Phi_i^t]$

$$\nabla_{h_{m,i}^t} \hat{f}_i^t = \nabla_{h_{m,i}^t} f_i^t + \nabla_{h_{m,i}^t}^2 f_i^t E_m^t + \dots \tag{34}$$

222 Define the infinite sum of all terms higher than the second partial derivative as  $R_n^t$ , where  $n$  denotes  
223 the number of terms in the remainder  $R$ :

$$R_n^t(w_0, h_{1,i} + \epsilon_{1,i}, \dots, h_{M,i} + \epsilon_{M,i}) = \nabla_{h_{m,i}^t}^2 f_i^t E_m^t + \dots \tag{35}$$

224 Therefore, for  $m = [M]$ ,

$$\begin{aligned}
&\mathbb{E} \left\| \nabla_{w_m} \hat{f}_i^t(w_0^t, \Phi_i^t) - \nabla_{w_m} f_i^t(w_0^t, \Phi_i^t) \right\|^2 \\
&= \mathbb{E} \left\| \nabla_{w_m} h_{m,i}^t \cdot R_0^t \right\|^2 \\
&\leq \mathbb{E} \left\| \nabla_{w_m} h_{m,i}^t \right\|^2 \left\| R_0^t \right\|^2 \\
&\stackrel{1)}{\leq} \mathbb{E} \mathbf{G}_m^2 \left\| R_0^t \right\|^2 \\
&\stackrel{2)}{\leq} \mathbf{G}_m^2 H_m^2 \mathbb{E} \left\| E_m^t \right\|^2 \\
&\stackrel{3)}{=} \mathbf{G}_m^2 H_m^2 \sum_{m=1}^M \mathcal{E}_m^t \\
&\stackrel{4)}{=} \mathbf{G}_m^2 H_m^2 \mathcal{E}^t \\
&\stackrel{5)}{\leq} \mathbf{G}_m^2 H_m^2 \mathcal{E}
\end{aligned} \tag{36}$$

225 where 1) apply assumption B.6, 2) apply the assumption B.5 and Taylor's inequality. 3) note that  
226 the specific error to be plugged in is  $E_m^t = [0, \epsilon_1^t, \dots, \epsilon_M^t]$ , i.e. the error for the  $w_0$  is 0, 4) for  
227 brevity, we use  $\mathcal{E}^t$  to denote  $\sum_{m=1}^M \|\mathcal{E}_m^t\|^2$  5) To make a succinct bound, let  $\mathcal{E} = \max_t \{\mathcal{E}^t\}$  denote  
228 the maximum norm of the error caused by the compression.

229 For the server  $\mathbb{E} \left\| \nabla_{w_0} \hat{f}_i^t(w_0^t, \Phi_i^t) - \nabla_{w_0} f_i^t(w_0^t, \Phi_i^t) \right\|^2$ , the  $w_0$  in  $f_i(w_0, \Phi_i)$  can be regarded as  $w_0$   
230 applying the identical function  $h_0(\cdot)$ , i.e.  $h_0(w_0) = w_0$ , and passing through the same procedures  
231 above. Note that  $\|\nabla_{w_0} h_0(w_0)\|^2 = 1$ .

$$\mathbb{E} \left\| \nabla_{w_0} \hat{f}_i^t(w_0^t, \Phi_i^t) - \nabla_{w_0} f_i^t(w_0^t, \Phi_i^t) \right\|^2$$

$$\begin{aligned}
&= \mathbb{E} \left\| \nabla_{w_0} h_0^t \cdot R_0^t \right\|^2 \\
&\leq \mathbb{E} \left\| \nabla_{w_0} h_0^t \right\|^2 \left\| R_0^t \right\|^2 \\
&\leq \mathbb{E} \left\| R_0^t \right\|^2 \\
&\leq H_0^2 \mathbb{E} \left\| E_m^t \right\|^2 \\
&= H_0^2 \sum_{m=1}^M \mathcal{E}_m^t \\
&= H_0^2 \mathcal{E}^t \\
&\leq H_0^2 \mathcal{E}
\end{aligned} \tag{37}$$

#### 232 D.4 Bound the Global Update Round

233 In one global round during training, the client  $m_t$  is activated, and the server and the client  $m_t$  update  
234 one step. Taking expectations w.r.t. the sample  $i$  and the random direction  $u$  for the zeroth-order  
235 optimization in one global update round.

$$\begin{aligned}
&\mathbb{E}_{i,u} \left[ f(w_0^{t+1}, w_1^t, \dots, w_{m_t}^{t+1}, \dots, w_M^t) - f(w_0^t, w_1^t, \dots, w_{m_t}^t, \dots, w_M^t) \right] \\
&\stackrel{1)}{\leq} \underbrace{-\eta_0 \mathbb{E}_i \left\langle \nabla_{w_0} f(w_0^t, \mathbf{w}^t), \nabla_{w_0} \hat{f}_i(w_0^t, \tilde{\Phi}_i^t) \right\rangle}_{a)} \\
&\quad + \underbrace{\frac{1}{2} L \eta_0^2 \mathbb{E}_i \left\| \nabla_{w_0} \hat{f}_i(w_0^t, \tilde{\Phi}_i^t) \right\|^2}_{b)} \\
&\quad - \underbrace{\eta_{m_t} \mathbb{E}_{i,u} \left\langle \nabla_{w_{m_t}} f(w_0^t, \mathbf{w}^t), \hat{\nabla}_{h_{m_t}} \hat{f}_i(w_0^t, \tilde{\Phi}_i(w_{m_t}^t)) \nabla_{w_{m_t}} h_{m_t}(w_{m_t}^t; x_{m_t,i}) \right\rangle}_{c)} \\
&\quad + \underbrace{\frac{1}{2} L \eta_{m_t}^2 \mathbb{E}_{i,u} \left\| \hat{\nabla}_{h_{m_t}} \hat{f}_i(w_0^t, \tilde{\Phi}_i(w_{m_t}^t)) \nabla_{w_{m_t}} h_{m_t}(w_{m_t}^t; x_{m_t,i}) \right\|^2}_{d)} \\
&\stackrel{2)}{\leq} -\frac{1}{2} \eta_0 \mathbb{E}_i \left\| \nabla_{w_0} f(w_0^t, \mathbf{w}^t) \right\|^2 + \eta_0 H_0^2 \mathcal{E} + \eta_0 L_0^2 \mathbb{E}_i \left\| \tilde{\mathbf{w}}^t - \mathbf{w}^t \right\|^2 \\
&\quad + L \eta_0^2 \mathbb{E}_i \left\| \nabla_{w_0} f(w_0^t, \mathbf{w}^t) \right\|^2 + L \eta_0^2 \sigma_0^2 + 2L \eta_0^2 H_0^2 \mathcal{E} + 2L \eta_0^2 L_0^2 \mathbb{E}_i \left\| \tilde{\mathbf{w}}^t - \mathbf{w}^t \right\|^2 \\
&\quad - \frac{1}{2} \eta_{m_t} \left\| \nabla_{w_{m_t}} f(\cdot) \right\|^2 + \frac{1}{4} \eta_{m_t} \mu_{m_t}^2 L_{m_t}^2 d_{h_{m_t}}^2 \mathbf{G}_{m_t}^2 + 4\eta_{m_t} \mathbf{G}_{m_t}^2 H_{m_t}^2 \mathcal{E} + 2\eta_{m_t} L_{m_t}^2 \mathbb{E}_i \left\| \tilde{\mathbf{w}}^t - \mathbf{w}^t \right\|^2 \\
&\quad + 4\eta_{m_t} \Gamma \mathbf{G}_{m_t}^2 \\
&\quad + 2L \eta_{m_t}^2 d_{h_{m_t}} \mathbf{G}_0^2 \mathbf{G}_{m_t}^2 + \frac{1}{2} L \eta_{m_t}^2 \mu_{m_t}^2 L_{m_t}^2 d_{h_{m_t}}^2 \mathbf{G}_{m_t}^2 + L \eta_{m_t}^2 \mathbf{G}_{m_t}^2 \Gamma \\
&\stackrel{3)}{\leq} -\left( \frac{1}{2} \eta_0 - L \eta_0^2 \right) \mathbb{E}_i \left\| \nabla_{w_0} f(w_0^t, \mathbf{w}^t) \right\|^2 - \frac{1}{2} \eta_{m_t} \mathbb{E}_i \left\| \nabla_{w_{m_t}} f(w_0^t, \mathbf{w}^t) \right\|^2 \\
&\quad + (\eta_0 L_0^2 + 2L \eta_0^2 L_0^2 + 2\eta_{m_t} L_{m_t}^2) \mathbb{E}_i \left\| \tilde{\mathbf{w}}^t - \mathbf{w}^t \right\|^2 \\
&\quad + \eta_0 H_0^2 \mathcal{E} + 2L \eta_0^2 H_0^2 \mathcal{E} + 4\eta_{m_t} \mathbf{G}_{m_t}^2 H_{m_t}^2 \mathcal{E} + 4\eta_{m_t} \mathbf{G}_{m_t}^2 \Gamma + L \eta_{m_t}^2 \mathbf{G}_{m_t}^2 \Gamma \\
&\quad + \frac{1}{4} \eta_{m_t} \mu_{m_t}^2 L_{m_t}^2 d_{h_{m_t}}^2 \mathbf{G}_{m_t}^2 + 2L \eta_{m_t}^2 d_{h_{m_t}} \mathbf{G}_0^2 \mathbf{G}_{m_t}^2 + \frac{1}{2} L \eta_{m_t}^2 \mu_{m_t}^2 L_{m_t}^2 d_{h_{m_t}}^2 \mathbf{G}_{m_t}^2 \\
&\quad + L \eta_0^2 \sigma_0^2
\end{aligned} \tag{38}$$

236 where 1) applies assumption B.2 (smoothness). Then we will discuss the server's update (a&b) and  
237 the client's update (c&d) separately in the following paragraph. 2) plugging in a), b), c) and d). 3)  
238 organize the equation.

239 for a)

$$\begin{aligned}
& -\eta_0 \mathbb{E}_i \left\langle \nabla_{w_0} f(w_0^t, \mathbf{w}^t), \nabla_{w_0} \hat{f}_i(w_0^t, \tilde{\Phi}_i^t) \right\rangle \\
& \stackrel{0)}{=} -\eta_0 \mathbb{E}_i \left\langle \nabla_{w_0} f(w_0^t, \mathbf{w}^t), \nabla_{w_0} \hat{f}_i(\tilde{\Phi}_i^t) \right\rangle \\
& = -\eta_0 \mathbb{E}_i \left\langle \nabla_{w_0} f(w_0^t, \mathbf{w}^t), \nabla_{w_0} \hat{f}_i(\tilde{\Phi}_i^t) - \nabla_{w_0} f_i(\Phi_i^t) + \nabla_{w_0} f_i(\Phi_i^t) \right\rangle \\
& = \eta_0 \mathbb{E}_i \left\langle -\nabla_{w_0} f(w_0^t, \mathbf{w}^t), \nabla_{w_0} \hat{f}_i(\tilde{\Phi}_i^t) - \nabla_{w_0} f_i(\Phi_i^t) \right\rangle - \eta_0 \mathbb{E}_i \left\langle \nabla_{w_0} f(w_0^t, \mathbf{w}^t), \nabla_{w_0} f_i(\Phi_i^t) \right\rangle \\
& \stackrel{1)}{=} \eta_0 \mathbb{E}_i \left\langle -\nabla_{w_0} f(w_0^t, \mathbf{w}^t), \nabla_{w_0} \hat{f}_i(\tilde{\Phi}_i^t) - \nabla_{w_0} f_i(\Phi_i^t) \right\rangle - \eta_0 \mathbb{E}_i \|\nabla_{w_0} f(w_0^t, \mathbf{w}^t)\|^2 \\
& \stackrel{2)}{\leq} -\frac{1}{2} \eta_0 \mathbb{E}_i \|\nabla_{w_0} f(w_0^t, \mathbf{w}^t)\|^2 + \frac{1}{2} \eta_0 \mathbb{E}_i \left\| \nabla_{w_0} \hat{f}_i(\tilde{\Phi}_i^t) - \nabla_{w_0} f_i(\Phi_i^t) \right\|^2 \\
& = -\frac{1}{2} \eta_0 \mathbb{E}_i \|\nabla_{w_0} f(w_0^t, \mathbf{w}^t)\|^2 \\
& \quad + \frac{1}{2} \eta_0 \mathbb{E}_i \left\| \nabla_{w_0} \hat{f}_i(\tilde{\Phi}_i^t) - \nabla_{w_0} f_i(\tilde{\Phi}_i^t) + \nabla_{w_0} f_i(\tilde{\Phi}_i^t) - \nabla_{w_0} f_i(\Phi_i^t) \right\|^2 \\
& \stackrel{3)}{\leq} -\frac{1}{2} \eta_0 \mathbb{E}_i \|\nabla_{w_0} f(w_0^t, \mathbf{w}^t)\|^2 \\
& \quad + \eta_0 \mathbb{E}_i \left\| \nabla_{w_0} \hat{f}_i(\tilde{\Phi}_i^t) - \nabla_{w_0} f_i(\tilde{\Phi}_i^t) \right\|^2 + \eta_0 \mathbb{E}_i \left\| \nabla_{w_0} f_i(\tilde{\Phi}_i^t) - \nabla_{w_0} f_i(\Phi_i^t) \right\|^2 \\
& \stackrel{4)}{\leq} -\frac{1}{2} \eta_0 \mathbb{E}_i \|\nabla_{w_0} f(w_0^t, \mathbf{w}^t)\|^2 + \eta_0 H_0^2 \mathcal{E} + \eta_0 L_0^2 \mathbb{E}_i \|\tilde{\mathbf{w}}^t - \mathbf{w}^t\|^2
\end{aligned} \tag{39}$$

240 where 0) For notation brevity, we mark  $f_i(w_0^t, \tilde{\Phi}_i^t)$  as  $f_i(\tilde{\Phi}_i^t)$ , (omit the common parameters), 1)  
241 applies assumption B.3 (unbiased gradient), 2)  $\langle a, b \rangle \leq \frac{1}{2} \|a\|^2 + \frac{1}{2} \|b\|^2$ , 3)  $\|a + b\|^2 \leq 2 \|a\|^2 +$   
242  $2 \|b\|^2$ , 4) lemma D.4 and assumption B.2 (smoothness).

243 for b)

$$\begin{aligned}
& \frac{1}{2} \mathbb{E}_i \left\| \nabla_{w_0} \hat{f}_i(w_0^t, \tilde{\Phi}_i^t) \right\|^2 \\
& \stackrel{0)}{=} \frac{1}{2} \mathbb{E}_i \left\| \nabla_{w_0} \hat{f}_i(\tilde{\Phi}_i^t) - \nabla_{w_0} f_i(\Phi_i^t) + \nabla_{w_0} f_i(\Phi_i^t) \right\|^2 \\
& \stackrel{1)}{\leq} \mathbb{E}_i \left\| \nabla_{w_0} \hat{f}_i(\tilde{\Phi}_i^t) - \nabla_{w_0} f_i(\Phi_i^t) \right\|^2 + \mathbb{E}_i \|\nabla_{w_0} f_i(\Phi_i^t)\|^2 \\
& \stackrel{2)}{\leq} \mathbb{E}_i \left\| \nabla_{w_0} \hat{f}_i(\tilde{\Phi}_i^t) - \nabla_{w_0} f_i(\Phi_i^t) \right\|^2 + \mathbb{E}_i \|\nabla_{w_0} f(\mathbf{w}^t)\|^2 + \sigma_0^2 \\
& = \mathbb{E}_i \|\nabla_{w_0} f(\mathbf{w}^t)\|^2 + \sigma_0^2 \\
& \quad + \mathbb{E}_i \left\| \nabla_{w_0} \hat{f}_i(\tilde{\Phi}_i^t) - \nabla_{w_0} f_i(\tilde{\Phi}_i^t) + \nabla_{w_0} f_i(\tilde{\Phi}_i^t) - \nabla_{w_0} f_i(\Phi_i^t) \right\|^2 \\
& \stackrel{3)}{\leq} \mathbb{E}_i \|\nabla_{w_0} f(\mathbf{w}^t)\|^2 + \sigma_0^2 \\
& \quad + 2 \mathbb{E}_i \left\| \nabla_{w_0} \hat{f}_i(\tilde{\Phi}_i^t) - \nabla_{w_0} f_i(\tilde{\Phi}_i^t) \right\|^2 + 2 \mathbb{E}_i \left\| \nabla_{w_0} f_i(\tilde{\Phi}_i^t) - \nabla_{w_0} f_i(\Phi_i^t) \right\|^2 \\
& \stackrel{4)}{\leq} \mathbb{E}_i \|\nabla_{w_0} f(\mathbf{w}^t)\|^2 + \sigma_0^2 + 2H_0^2 \mathcal{E} + 2L_0^2 \mathbb{E}_i \|\tilde{\mathbf{w}}^t - \mathbf{w}^t\|^2
\end{aligned} \tag{40}$$

244 where 0) For notation brevity, we mark  $f_i(w_0^t, \tilde{\Phi}_i^t)$  as  $f_i(\tilde{\Phi}_i^t)$ , (omit the common parame-  
245 ters), 1) applies  $\|a + b\|^2 \leq 2 \|a\|^2 + 2 \|b\|^2$ , 2) applies  $\mathbb{E}(X^2) = \mathbb{E}(X)^2 + \text{Var}(X)$ , assump-  
246 tion B.3 (unbiased gradient) and assumption B.4 (bounded variance), i.e.  $\mathbb{E}_i \|\nabla_{w_0} f_i(\Phi_i^t)\|^2 =$

247  $\|\nabla_{w_0} f(\Phi_i^t)\|^2 + \text{Var}(\nabla_{w_0} f_i(\Phi_i)) \leq \|\nabla_{w_0} f(\mathbf{w}^t)\|^2 + \sigma_0^2$ , 3) applies  $\|a + b\|^2 \leq 2\|a\|^2 + 2\|b\|^2$ ,  
 248 4) lemma D.4 and assumption B.2 (smoothness).

249 then b) is

$$\begin{aligned} & L\eta_0^2 \left( \frac{1}{2} \mathbb{E}_i \left\| \nabla_{w_0} \hat{f}_i \left( w_0^t, \tilde{\Phi}_i^t \right) \right\|^2 \right) \\ &= L\eta_0^2 \mathbb{E}_i \left\| \nabla_{w_0} f(\mathbf{w}^t) \right\|^2 + L\eta_0^2 \sigma_0^2 + 2L\eta_0^2 H_0^2 \mathcal{E} + 2L\eta_0^2 L_0^2 \mathbb{E}_i \left\| \tilde{\mathbf{w}}^t - \mathbf{w}^t \right\|^2 \end{aligned} \quad (41)$$

250 for c)

$$\begin{aligned} & -\eta_{m_t} \mathbb{E}_{i,u} \left\langle \nabla_{w_{m_t}} f(w_0^t, \mathbf{w}^t), \left[ \hat{\nabla}_{h_{m_t,i}^t} \hat{f}_i \left( w_0^t, \tilde{\Phi}_i(w_{m_t}^t) \right) + \gamma^t \right] \cdot \nabla_{w_{m_t}} h_{m_t}(w_{m_t}^t; x_{m_t,i}) \right\rangle \\ & \stackrel{0)}{=} -\eta_{m_t} \mathbb{E}_{i,u} \left\langle \nabla_{w_{m_t}} f(\cdot), \left[ \hat{\nabla}_{h_{m_t,i}^t} \hat{f}_i \left( \tilde{\Phi}_i(w_{m_t}^t) \right) + \gamma^t \right] \cdot \nabla_{w_{m_t}} h_{m_t,i}^t \right\rangle \\ & \stackrel{1)}{=} -\eta_{m_t} \mathbb{E}_i \left\langle \nabla_{w_{m_t}} f(\cdot), \nabla_{h_{m_t,i}^t} \hat{f}_{\mu_{m_t,i}} \left( \tilde{\Phi}_i(w_{m_t}^t) \right) \cdot \nabla_{w_{m_t}} h_{m_t,i}^t + \gamma^t \cdot \nabla_{w_{m_t}} h_{m_t,i}^t \right\rangle \\ & = -\eta_{m_t} \mathbb{E}_i \left\langle \nabla_{w_{m_t}} f(\cdot), \nabla_{h_{m_t,i}^t} \hat{f}_{\mu_{m_t,i}} \left( \tilde{\Phi}_i(w_{m_t}^t) \right) \cdot \nabla_{w_{m_t}} h_{m_t,i}^t + \gamma^t \cdot \nabla_{w_{m_t}} h_{m_t,i}^t - \nabla_{w_{m_t}} f_i \left( \Phi_i(w_{m_t}^t) \right) \right. \\ & \quad \left. + \nabla_{w_{m_t}} f_i \left( \Phi_i(w_{m_t}^t) \right) \right\rangle \\ & = \eta_{m_t} \mathbb{E}_i \left\langle -\nabla_{w_{m_t}} f(\cdot), \nabla_{h_{m_t,i}^t} \hat{f}_{\mu_{m_t,i}} \left( \tilde{\Phi}_i(w_{m_t}^t) \right) \cdot \nabla_{w_{m_t}} h_{m_t,i}^t - \nabla_{w_{m_t}} f_i \left( \Phi_i(w_{m_t}^t) \right) + \gamma^t \cdot \nabla_{w_{m_t}} h_{m_t,i}^t \right\rangle \\ & \quad - \eta_{m_t} \mathbb{E}_i \left\langle \nabla_{w_{m_t}} f(\cdot), \nabla_{w_{m_t}} f_i \left( \Phi_i(w_{m_t}^t) \right) \right\rangle \\ & \stackrel{2)}{=} \eta_{m_t} \mathbb{E}_i \left\langle -\nabla_{w_{m_t}} f(\cdot), \nabla_{h_{m_t,i}^t} \hat{f}_{\mu_{m_t,i}} \left( \tilde{\Phi}_i(w_{m_t}^t) \right) \cdot \nabla_{w_{m_t}} h_{m_t,i}^t - \nabla_{w_{m_t}} f_i \left( \Phi_i(w_{m_t}^t) \right) + \gamma^t \cdot \nabla_{w_{m_t}} h_{m_t,i}^t \right\rangle \\ & \quad - \eta_{m_t} \mathbb{E}_i \left\| \nabla_{w_{m_t}} f(\cdot) \right\|^2 \\ & \stackrel{3)}{\leq} -\frac{1}{2} \eta_{m_t} \left\| \nabla_{w_{m_t}} f(\cdot) \right\|^2 \\ & \quad + \frac{1}{2} \eta_{m_t} \mathbb{E}_i \left\| \nabla_{h_{m_t,i}^t} \hat{f}_{\mu_{m_t,i}} \left( \tilde{\Phi}_i(w_{m_t}^t) \right) \cdot \nabla_{w_{m_t}} h_{m_t,i}^t - \nabla_{w_{m_t}} f_i \left( \Phi_i(w_{m_t}^t) \right) + \gamma^t \cdot \nabla_{w_{m_t}} h_{m_t,i}^t \right\|^2 \\ & = -\frac{1}{2} \eta_{m_t} \left\| \nabla_{w_{m_t}} f(\cdot) \right\|^2 \\ & \quad + \frac{1}{2} \eta_{m_t} \mathbb{E}_i \left\| \nabla_{h_{m_t,i}^t} \hat{f}_{\mu_{m_t,i}} \left( \tilde{\Phi}_i(w_{m_t}^t) \right) \cdot \nabla_{w_{m_t}} h_{m_t,i}^t - \nabla_{w_{m_t}} \hat{f}_i \left( \tilde{\Phi}_i(w_{m_t}^t) \right) + \nabla_{w_{m_t}} \hat{f}_i \left( \tilde{\Phi}_i(w_{m_t}^t) \right) \right. \\ & \quad \left. - \nabla_{w_{m_t}} f_i \left( \tilde{\Phi}_i(w_{m_t}^t) \right) + \nabla_{w_{m_t}} f_i \left( \tilde{\Phi}_i(w_{m_t}^t) \right) - \nabla_{w_{m_t}} f_i \left( \Phi_i(w_{m_t}^t) \right) + \gamma^t \cdot \nabla_{w_{m_t}} h_{m_t,i}^t \right\|^2 \\ & \stackrel{4)}{\leq} -\frac{1}{2} \eta_{m_t} \left\| \nabla_{w_{m_t}} f(\cdot) \right\|^2 \\ & \quad + \eta_{m_t} \mathbb{E}_i \left\| \nabla_{h_{m_t,i}^t} \hat{f}_{\mu_{m_t,i}} \left( \tilde{\Phi}_i(w_{m_t}^t) \right) \cdot \nabla_{w_{m_t}} h_{m_t,i}^t - \nabla_{w_{m_t}} \hat{f}_i \left( \tilde{\Phi}_i(w_{m_t}^t) \right) \right\|^2 \\ & \quad + 4\eta_{m_t} \mathbb{E}_i \left\| \nabla_{w_{m_t}} \hat{f}_i \left( \tilde{\Phi}_i(w_{m_t}^t) \right) - \nabla_{w_{m_t}} f_i \left( \tilde{\Phi}_i(w_{m_t}^t) \right) \right\|^2 + 4\eta_{m_t} \mathbb{E}_i \left\| \gamma^t \cdot \nabla_{w_{m_t}} h_{m_t,i}^t \right\|^2 \\ & \quad + 2\eta_{m_t} \mathbb{E}_i \left\| \nabla_{w_{m_t}} \hat{f}_i \left( \tilde{\Phi}_i(w_{m_t}^t) \right) - \nabla_{w_{m_t}} f_i \left( \Phi_i(w_{m_t}^t) \right) \right\|^2 \\ & \leq -\frac{1}{2} \eta_{m_t} \left\| \nabla_{w_{m_t}} f(\cdot) \right\|^2 \\ & \quad + \eta_{m_t} \mathbb{E}_i \left\| \nabla_{h_{m_t,i}^t} \hat{f}_{\mu_{m_t,i}} \left( \tilde{\Phi}_i(w_{m_t}^t) \right) - \nabla_{h_{m_t,i}^t} \hat{f}_i \left( \tilde{\Phi}_i(w_{m_t}^t) \right) \right\|^2 \left\| \nabla_{w_{m_t}} h_{m_t,i}^t \right\|^2 \\ & \quad + 4\eta_{m_t} \mathbb{E}_i \left\| \nabla_{w_{m_t}} \hat{f}_i \left( \tilde{\Phi}_i(w_{m_t}^t) \right) - \nabla_{w_{m_t}} f_i \left( \tilde{\Phi}_i(w_{m_t}^t) \right) \right\|^2 + 4\eta_{m_t} \mathbb{E}_i \left\| \gamma^t \cdot \nabla_{w_{m_t}} h_{m_t,i}^t \right\|^2 \\ & \quad + 2\eta_{m_t} \mathbb{E}_i \left\| \nabla_{w_{m_t}} \hat{f}_i \left( \tilde{\Phi}_i(w_{m_t}^t) \right) - \nabla_{w_{m_t}} f_i \left( \Phi_i(w_{m_t}^t) \right) \right\|^2 \\ & \stackrel{5)}{\leq} -\frac{1}{2} \eta_{m_t} \left\| \nabla_{w_{m_t}} f(\cdot) \right\|^2 + \eta_{m_t} \frac{\mu_{m_t}^2 L_{m_t}^2 d_{h_{m_t}}^2}{4} \mathbf{G}_{m_t}^2 \end{aligned}$$

$$\begin{aligned}
& + 4\eta_{m_t} \mathbb{E}_i \left\| \nabla_{w_{m_t}} \hat{f}_i \left( \tilde{\Phi}_i(w_{m_t}^t) \right) - \nabla_{w_{m_t}} f_i \left( \tilde{\Phi}_i(w_{m_t}^t) \right) \right\|^2 + 4\eta_{m_t} \mathbb{E}_i \left\| \gamma^t \cdot \nabla_{w_{m_t}} h_{m_t,i}^t \right\|^2 \\
& + 2\eta_{m_t} \mathbb{E}_i \left\| \nabla_{w_{m_t}} \hat{f}_i \left( \tilde{\Phi}_i(w_{m_t}^t) \right) - \nabla_{w_{m_t}} f_i \left( \Phi_i(w_{m_t}^t) \right) \right\|^2 \\
& \stackrel{6)}{\leq} -\frac{1}{2} \eta_{m_t} \left\| \nabla_{w_{m_t}} f(\cdot) \right\|^2 + \frac{1}{4} \eta_{m_t} \mu_{m_t}^2 L_{m_t}^2 d_{h_{m_t}}^2 \mathbf{G}_{m_t}^2 + 4\eta_{m_t} \mathbf{G}_{m_t}^2 H_{m_t}^2 \mathcal{E} + 2\eta_{m_t} L_{m_t}^2 \mathbb{E}_i \left\| \tilde{\mathbf{w}}^t - \mathbf{w}^t \right\|^2 \\
& \quad + 4\eta_{m_t} \mathbb{E}_i \left\| \gamma^t \cdot \nabla_{w_{m_t}} h_{m_t,i}^t \right\|^2 \\
& \leq -\frac{1}{2} \eta_{m_t} \left\| \nabla_{w_{m_t}} f(\cdot) \right\|^2 + \frac{1}{4} \eta_{m_t} \mu_{m_t}^2 L_{m_t}^2 d_{h_{m_t}}^2 \mathbf{G}_{m_t}^2 + 4\eta_{m_t} \mathbf{G}_{m_t}^2 H_{m_t}^2 \mathcal{E} + 2\eta_{m_t} L_{m_t}^2 \mathbb{E}_i \left\| \tilde{\mathbf{w}}^t - \mathbf{w}^t \right\|^2 \\
& \quad + 4\eta_{m_t} \mathbb{E}_i \left\| \gamma^t \right\|^2 \left\| \nabla_{w_{m_t}} h_{m_t,i}^t \right\|^2 \\
& \stackrel{7)}{\leq} -\frac{1}{2} \eta_{m_t} \left\| \nabla_{w_{m_t}} f(\cdot) \right\|^2 + \frac{1}{4} \eta_{m_t} \mu_{m_t}^2 L_{m_t}^2 d_{h_{m_t}}^2 \mathbf{G}_{m_t}^2 + 4\eta_{m_t} \mathbf{G}_{m_t}^2 H_{m_t}^2 \mathcal{E} + 2\eta_{m_t} L_{m_t}^2 \mathbb{E}_i \left\| \tilde{\mathbf{w}}^t - \mathbf{w}^t \right\|^2 \\
& \quad + 4\eta_{m_t} \Gamma \mathbf{G}_{m_t}^2
\end{aligned} \tag{42}$$

251 where 0) for notation brevity, we omit the common parameters,  $f(w_0^t, \mathbf{w}^t) = f(\cdot)$ ,  
252  $\hat{f}_i(w_0^t, \tilde{\Phi}_i(w_{m_t}^t)) = \hat{f}_i(\tilde{\Phi}_i(w_{m_t}^t))$ ,  $h_{m_t}(w_{m_t}^t; x_{m_t,i}) = h_{m_t,i}^t$ , 1) applies Eq.26 in  
253 lemma D.3, 2) applies assumption B.3 (unbiased gradient) and we use  $f(w_{m_t}^t)$  to denote  
254  $f(w_0^{t,0}, w_1^{t,0}, \dots, w_{m_t}^t, \dots, w_M^{t,0})$ , 3)  $\langle a, b \rangle \leq \frac{1}{2} \|a\|^2 + \frac{1}{2} \|b\|^2$ , 4) applying  $\|a + b\|^2 \leq 2\|a\|^2 +$   
255  $2\|b\|^2$  recursively, 5) applies Eq. 28 in lemma D.3 and the assumption B.6 (bounded block-  
256 coordinated gradient), 6) applies lemma D.4 and assumption B.2. 7) applies assumption B.6 (bounded  
257 block-coordinated gradient) and definition D.2.

258 for d)

$$\begin{aligned}
& \frac{1}{2} \mathbb{E}_{i,u} \left\| \left[ \hat{\nabla}_{h_{m_t}} \hat{f}_i \left( w_0^t, \tilde{\Phi}(w_{m_t}^t) \right) + \gamma^t \right] \cdot \nabla_{w_{m_t}} h_{m_t}(w_{m_t}^t; x_{m_t,i}) \right\|^2 \\
& \stackrel{0)}{=} \frac{1}{2} \mathbb{E}_{i,u} \left\| \left[ \hat{\nabla}_{h_{m_t}} \hat{f}_i \left( \tilde{\Phi}(w_{m_t}^t) \right) + \gamma^t \right] \cdot \nabla_{w_{m_t}} h_{m_t,i}^t \right\|^2 \\
& \leq \frac{1}{2} \mathbb{E}_{i,u} \left\| \hat{\nabla}_{h_{m_t}} \hat{f}_i \left( \tilde{\Phi}(w_{m_t}^t) \right) + \gamma^t \right\|^2 \left\| \nabla_{w_{m_t}} h_{m_t,i}^t \right\|^2 \\
& \stackrel{1)}{\leq} \mathbb{E}_{i,u} \left\| \hat{\nabla}_{h_{m_t}} \hat{f}_i \left( \tilde{\Phi}(w_{m_t}^t) \right) \right\|^2 \left\| \nabla_{w_{m_t}} h_{m_t,i}^t \right\|^2 + \mathbb{E}_{i,u} \left\| \gamma^t \right\|^2 \left\| \nabla_{w_{m_t}} h_{m_t,i}^t \right\|^2 \\
& \stackrel{2)}{\leq} \mathbf{G}_{m_t}^2 \mathbb{E}_{i,u} \left\| \hat{\nabla}_{h_{m_t}} \hat{f}_i \left( \tilde{\Phi}(w_{m_t}^t) \right) \right\|^2 + \mathbb{E}_{i,u} \left\| \gamma^t \right\|^2 \mathbf{G}_{m_t}^2 \\
& \stackrel{3)}{\leq} \mathbf{G}_{m_t}^2 \left( 2d_{h_{m_t}} \left\| \nabla_{h_{m_t}} \hat{f}_i \left( \tilde{\Phi}(w_{m_t}^t) \right) \right\|^2 + \frac{1}{2} \mu_{m_t}^2 L_{m_t}^2 d_{h_{m_t}}^2 \right) + \mathbb{E}_{i,u} \left\| \gamma^t \right\|^2 \mathbf{G}_{m_t}^2 \\
& = 2\mathbf{G}_{m_t}^2 d_{h_{m_t}} \left\| \nabla_{h_{m_t}} \hat{f}_i \left( \tilde{\Phi}(w_{m_t}^t) \right) \right\|^2 + \frac{1}{2} \mu_{m_t}^2 L_{m_t}^2 d_{h_{m_t}}^2 \mathbf{G}_{m_t}^2 + \mathbb{E}_{i,u} \left\| \gamma^t \right\|^2 \mathbf{G}_{m_t}^2 \\
& \stackrel{4)}{\leq} 2d_{h_{m_t}} \mathbf{G}_0^2 \mathbf{G}_{m_t}^2 + \frac{1}{2} \mu_{m_t}^2 L_{m_t}^2 d_{h_{m_t}}^2 \mathbf{G}_{m_t}^2 + \Gamma \mathbf{G}_{m_t}^2
\end{aligned} \tag{43}$$

259 where 0) for notation brevity, we omit the common parameters, i.e.  $f(w_0^t, \mathbf{w}^t) = f(\cdot)$ ,  
260  $\hat{f}_i(w_0^t, \tilde{\Phi}_i(w_{m_t}^t)) = \hat{f}_i(\tilde{\Phi}_i(w_{m_t}^t))$ ,  $h_{m_t}(w_{m_t}^t; x_{m_t,i}) = h_{m_t,i}^t$ , 1) applies  $\|a + b\|^2 \leq 2\|a\|^2 +$   
261  $2\|b\|^2$ , 2) applies assumption B.6 (bounded block-coordinated gradient), 3) applies Eq. 30 in  
262 lemma D.3, 4)  $\Gamma = \max_t \{\Gamma^t\}$ .

263 Then d) is

$$\begin{aligned}
& L\eta_{m_t}^2 \left( \frac{1}{2} \mathbb{E}_{i,u} \left\| \hat{\nabla}_{h_{m_t}} \hat{f}_i \left( w_0^t, \tilde{\Phi}(w_{m_t}^t) \right) \nabla_{w_{m_t}} h_{m_t}(w_{m_t}^t; x_{m_t,i}) \right\|^2 \right) \\
& \leq 2L\eta_{m_t}^2 d_{h_{m_t}} \mathbf{G}_0^2 \mathbf{G}_{m_t}^2 + \frac{1}{2} L\eta_{m_t}^2 \mu_{m_t}^2 L_{m_t}^2 d_{h_{m_t}}^2 \mathbf{G}_{m_t}^2 + L\eta_{m_t}^2 \Gamma \mathbf{G}_{m_t}^2
\end{aligned}$$

(44)

264 **D.5 Combine the Gradient**

265 Start with the Eq. 38, additionally taking expectation w.r.t. activated client  $m_t$ , and applying the  
 266 assumption B.7 (independent client).

$$\begin{aligned}
& \mathbb{E}_{m_t, i, u} [f(w_0^{t+1}, w_1^t, \dots, w_{m_t}^{t+1}, \dots, w_M^t) - f(w_0^t, w_1^t, \dots, w_{m_t}^t, \dots, w_M^t)] \\
& \leq - \left( \frac{1}{2} \eta_0 - L\eta_0^2 \right) \mathbb{E}_i \|\nabla_{w_0} f(w_0^t, \mathbf{w}^t)\|^2 - \frac{1}{2} \sum_{m=1}^M p_m \eta_m \mathbb{E}_i \|\nabla_{w_m} f(w_0^t, \mathbf{w}^t)\|^2 \\
& \quad + \left( \eta_0 L_0^2 + 2L\eta_0^2 L_0^2 + 2 \sum_{m=1}^M p_m \eta_m L_m^2 \right) \mathbb{E}_i \|\tilde{\mathbf{w}}^t - \mathbf{w}^t\|^2 \\
& \quad + \eta_0 H_0^2 \mathcal{E} + 2L\eta_0^2 H_0^2 \mathcal{E} + 4 \sum_{m=1}^M p_m \eta_m \mathbf{G}_m^2 H_m^2 \mathcal{E} + 4 \sum_{m=1}^M p_m \eta_m \mathbf{G}_m^2 \Gamma + L \sum_{m=1}^M p_m \eta_m^2 \mathbf{G}_m^2 \Gamma \\
& \quad + \frac{1}{4} \sum_{m=1}^M p_m \eta_m \mu_m^2 L_m^2 d_{h_m}^2 \mathbf{G}_m^2 + 2 \sum_{m=1}^M p_m L \eta_m^2 d_{h_m} \mathbf{G}_0^2 \mathbf{G}_m^2 + \frac{1}{2} \sum_{m=1}^M p_m L \eta_m^2 \mu_m^2 L_m^2 d_{h_m}^2 \mathbf{G}_m^2 \\
& \quad + L\eta_0^2 \sigma_0^2 \\
& \stackrel{1)}{\leq} - \left( \frac{1}{2} \eta_0 - L\eta_0^2 \right) \mathbb{E}_i \|\nabla_{w_0} f(w_0^t, \mathbf{w}^t)\|^2 - \frac{1}{2} \sum_{m=1}^M p_m \eta_m \mathbb{E}_i \|\nabla_{w_m} f(w_0^t, \mathbf{w}^t)\|^2 \\
& \quad + \left( \eta_0 L_0^2 + 2L\eta_0^2 L_0^2 + 2 \sum_{m=1}^M p_m \eta_m L_m^2 \right) \mathbb{E}_i \|\tilde{\mathbf{w}}^t - \mathbf{w}^t\|^2 \\
& \quad + Q_1 \\
& \stackrel{2)}{\leq} - \frac{1}{4} \eta_0 \mathbb{E}_i \|\nabla_{w_0} f(w_0^t, \mathbf{w}^t)\|^2 - \frac{1}{4} \sum_{m=1}^M p_m \eta_m \mathbb{E}_i \|\nabla_{w_m} f(w_0^t, \mathbf{w}^t)\|^2 \\
& \quad + \left( \eta_0 L_0^2 + 2L\eta_0^2 L_0^2 + 2 \sum_{m=1}^M p_m \eta_m L_m^2 \right) \mathbb{E}_i \|\tilde{\mathbf{w}}^t - \mathbf{w}^t\|^2 \\
& \quad + Q_1 \\
& \stackrel{3)}{\leq} - \frac{1}{4} \min \{ \eta_0, p_m \eta_m \} \mathbb{E}_i \|\nabla f(w_0^t, \mathbf{w}^t)\|^2 \\
& \quad + \left( \eta_0 L_0^2 + 2L\eta_0^2 L_0^2 + 2 \sum_{m=1}^M p_m \eta_m L_m^2 \right) \mathbb{E}_i \|\tilde{\mathbf{w}}^t - \mathbf{w}^t\|^2 \\
& \quad + Q_1
\end{aligned} \tag{45}$$

267 where 1) for notation brevity, denotes the line 3-5 (constants) as  $Q_1$ , 2) let  $\eta_0 \leq$   
 268  $\frac{1}{4L}$  then  $-\frac{1}{2}\eta_0 + L\eta_0^2 < -\frac{1}{4}\eta_0$ , and  $-\frac{1}{2} \sum_{m=1}^M p_m \eta_m \mathbb{E}_i \|\nabla_{w_m} f(w_0^t, \mathbf{w}^t)\|^2 \leq$   
 269  $-\frac{1}{4} \sum_{m=1}^M p_m \eta_m \mathbb{E}_i \|\nabla_{w_m} f(w_0^t, \mathbf{w}^t)\|^2$ , 3) uses the orthogonality of  $\nabla f$ , i.e.  $\|\nabla f(w_0, \mathbf{w})\|^2 =$   
 270  $\|\nabla_{w_0} f(w_0, \mathbf{w})\|^2 + \sum_{m=1}^M \|\nabla_{w_m} f(w_0, \mathbf{w})\|^2$ .

271 **D.6 Define the Lyapunov Function to Eliminate the Client's Delay.**

272 Define a Lyapunov function.

$$M^t = f(w_0^t, \mathbf{w}^t) + \sum_{i=1}^{\tau} \theta_i \|\mathbf{w}^{t+1-i} - \mathbf{w}^{t-i}\|^2 \tag{46}$$

273 Taking expectation w.r.t. the activated client  $m_t$ , sample index  $i$ , and the random direction  $u$ .

$$\begin{aligned}
& \mathbb{E} (M^{t+1} - M^t) \\
&= \mathbb{E} \left[ f(w_0^{t+1}, \mathbf{w}^{t+1}) + \sum_{i=1}^{\tau} \theta_i \|\mathbf{w}^{t+1+1-i} - \mathbf{w}^{t+1-i}\|^2 \right] - \mathbb{E} \left[ f(w_0^t, \mathbf{w}^t) + \sum_{i=1}^{\tau} \theta_i \|\mathbf{w}^{t+1-i} - \mathbf{w}^{t-i}\|^2 \right] \\
&= \mathbb{E} [f(w_0^{t+1}, \mathbf{w}^{t+1}) - f(w_0^t, \mathbf{w}^t)] + \sum_{i=1}^{\tau} \theta_i \mathbb{E} \|\mathbf{w}^{t+1+1-i} - \mathbf{w}^{t+1-i}\|^2 - \sum_{i=1}^{\tau} \theta_i \mathbb{E} \|\mathbf{w}^{t+1-i} - \mathbf{w}^{t-i}\|^2 \\
&\stackrel{1)}{\leq} -\frac{1}{4} \min \{\eta_0, p_m \eta_m\} \mathbb{E} \|\nabla f(w_0^t, \mathbf{w}^t)\|^2 + Q_1 \\
&\quad + \underbrace{\left( \eta_0 L_0^2 + 2L\eta_0^2 L_0^2 + 2 \sum_{m=1}^M p_m \eta_m L_m^2 \right) \mathbb{E} \|\tilde{\mathbf{w}}^t - \mathbf{w}^t\|^2}_a \\
&\quad + \underbrace{\sum_{i=1}^{\tau} \theta_i \mathbb{E} \|\mathbf{w}^{t+1+1-i} - \mathbf{w}^{t+1-i}\|^2 - \sum_{i=1}^{\tau} \theta_i \mathbb{E} \|\mathbf{w}^{t+1-i} - \mathbf{w}^{t-i}\|^2}_b \\
&\stackrel{2)}{\leq} -\frac{1}{4} \min \{\eta_0, p_m \eta_m\} \mathbb{E} \|\nabla f(w_0^t, \mathbf{w}^t)\|^2 + Q_1 \\
&\quad + \left( \eta_0 L_0^2 + 2L\eta_0^2 L_0^2 + 2 \sum_{m=1}^M p_m \eta_m L_m^2 \right) \tau \sum_{i=1}^{\tau} \mathbb{E} \|\mathbf{w}^{t+1-i} - \mathbf{w}^{t-i}\|^2 \\
&\quad + \theta_1 \mathbb{E} \|\mathbf{w}^{t+1} - \mathbf{w}^t\|^2 + \sum_{i=1}^{\tau-1} (\theta_{i+1} - \theta_i) \mathbb{E} \|\mathbf{w}^{t+1-i} - \mathbf{w}^{t-i}\|^2 - \theta_{\tau} \mathbb{E} \|\mathbf{w}^{t+1-\tau} - \mathbf{w}^{t-\tau}\|^2 \\
&\leq -\frac{1}{4} \min \{\eta_0, p_m \eta_m\} \mathbb{E} \|\nabla f(w_0^t, \mathbf{w}^t)\|^2 + Q_1 \\
&\quad + \theta_1 \mathbb{E} \|\mathbf{w}^{t+1} - \mathbf{w}^t\|^2 \\
&\quad + \sum_{i=1}^{\tau-1} \left( \theta_{i+1} - \theta_i + \eta_0 L_0^2 + 2L\eta_0^2 L_0^2 + 2 \sum_{m=1}^M p_m \eta_m L_m^2 \right) \mathbb{E} \|\mathbf{w}^{t+1-i} - \mathbf{w}^{t-i}\|^2 \\
&\quad - \left[ \theta_{\tau} - \left( \eta_0 L_0^2 + 2L\eta_0^2 L_0^2 + 2 \sum_{m=1}^M p_m \eta_m L_m^2 \right) \right] \mathbb{E} \|\mathbf{w}^{t+1-\tau} - \mathbf{w}^{t-\tau}\|^2
\end{aligned} \tag{47}$$

274 where 1) plugging in Eq. 45, 2) plugging in a) and b).

275 For a) in Eq. 47:

$$\mathbb{E} \|\tilde{\mathbf{w}}^t - \mathbf{w}^t\|^2 \stackrel{1)}{\leq} \mathbb{E} \left\| \sum_{i=1}^{\tau} (\mathbf{w}^{i+1} - \mathbf{w}^i) \right\|^2 \stackrel{2)}{\leq} \tau \sum_{i=1}^{\tau} \mathbb{E} \|\mathbf{w}^{t+1-i} - \mathbf{w}^{t-i}\|^2 \tag{48}$$

276 where 1) applies assumption B.8 (uniformly bounded delay), 2) applies Cauchy-Schwarz inequality,

277 i.e.  $\left( \sum_{i=0}^{n-1} x_i \right)^2 = \left( \sum_{i=0}^{n-1} 1 \cdot x_i \right)^2 \leq n \sum_{i=0}^{n-1} x_i^2$ .

278 For b) in Eq. 47:

$$\begin{aligned}
& \sum_{i=1}^{\tau} \theta_i \mathbb{E} \|\mathbf{w}^{t+1+1-i} - \mathbf{w}^{t+1-i}\|^2 - \sum_{i=1}^{\tau} \theta_i \mathbb{E} \|\mathbf{w}^{t+1-i} - \mathbf{w}^{t-i}\|^2 \\
&= \theta_1 \mathbb{E} \|\mathbf{w}^{t+1} - \mathbf{w}^t\|^2 + \sum_{i=1}^{\tau-1} (\theta_{i+1} - \theta_i) \mathbb{E} \|\mathbf{w}^{t+1-i} - \mathbf{w}^{t-i}\|^2 - \theta_{\tau} \mathbb{E} \|\mathbf{w}^{t+1-\tau} - \mathbf{w}^{t-\tau}\|^2 \tag{49}
\end{aligned}$$

279 Let  $\theta_1 \geq \tau \left( \eta_0 L_0^2 + 2L\eta_0^2 L_0^2 + 2 \sum_{m=1}^M p_m \eta_m L_m^2 \right)$  and design the recurrent relation for  $\theta_i$

$$\theta_{i+1} = \theta_i - \left( \eta_0 L_0^2 + 2L\eta_0^2 L_0^2 + 2 \sum_{m=1}^M p_m \eta_m L_m^2 \right) \quad (50)$$

280 It follows that

$$\theta_\tau - \left( \eta_0 L_0^2 + 2L\eta_0^2 L_0^2 + 2 \sum_{m=1}^M p_m \eta_m L_m^2 \right) = \theta_1 - \tau \left( \eta_0 L_0^2 + 2L\eta_0^2 L_0^2 + 2 \sum_{m=1}^M p_m \eta_m L_m^2 \right) \geq 0 \quad (51)$$

281 Applying Eq. 50 and Eq. 51 to Eq. 47

$$\begin{aligned} & \mathbb{E} (M^{t+1} - M^t) \\ & \leq -\frac{1}{4} \min \{ \eta_0, p_m \eta_m \} \mathbb{E} \|\nabla f(w_0^t, \mathbf{w}^t)\|^2 + Q_1 \\ & \quad + \tau \left( \eta_0 L_0^2 + 2L\eta_0^2 L_0^2 + 2 \sum_{m=1}^M p_m \eta_m L_m^2 \right) \underbrace{\mathbb{E} \|\mathbf{w}^{t+1} - \mathbf{w}^t\|^2}_{c)} \\ & \leq -\frac{1}{4} \min \{ \eta_0, p_m \eta_m \} \mathbb{E} \|\nabla f(w_0^t, \mathbf{w}^t)\|^2 + Q_1 \\ & \quad + \tau \left( \eta_0 L_0^2 + 2L\eta_0^2 L_0^2 + 2 \sum_{m=1}^M p_m \eta_m L_m^2 \right) \left( 2 \sum_{m=1}^M p_m \eta_m^2 d_{h_m} \mathbf{G}_0^2 \mathbf{G}_m^2 \right. \\ & \quad \left. + \frac{1}{2} \sum_{m=1}^M p_m \eta_m^2 \mu_m^2 L_m^2 d_{h_m}^2 \mathbf{G}_m^2 + \sum_{m=1}^M p_m \eta_m^2 \mathbf{G}_m^2 \Gamma \right) \\ & \stackrel{1)}{=} -\frac{1}{4} \min \{ \eta_0, p_m \eta_m \} \mathbb{E} \|\nabla f(w_0^t, \mathbf{w}^t)\|^2 + Q_1 + Q_2 \end{aligned} \quad (52)$$

282 where 1) mark the second line as  $Q_2$  for notation brevity.

283 For c),

$$\begin{aligned} & \mathbb{E}_{m_t, i, u} \|\mathbf{w}^{t+1} - \mathbf{w}^t\|^2 \\ & \stackrel{1)}{=} \mathbb{E}_{m_t, i, u} \left\| \eta_{m_t} \left[ \hat{\nabla}_{h_{m_t}} \hat{f}_i(w_0^t, \tilde{\Phi}(w_{m_t}^t)) + \gamma^t \right] \nabla_{w_{m_t}} h_{m_t}(w_{m_t}^t; x_{m_t, i}) \right\|^2 \\ & \stackrel{2)}{\leq} 2 \sum_{m=1}^M p_m \eta_m^2 d_{h_m} \mathbf{G}_0^2 \mathbf{G}_m^2 + \frac{1}{2} \sum_{m=1}^M p_m \eta_m^2 \mu_m^2 L_m^2 d_{h_m}^2 \mathbf{G}_m^2 + \sum_{m=1}^M p_m \eta_m^2 \mathbf{G}_m^2 \Gamma \end{aligned} \quad (53)$$

284 where 1) the update rule for the communication round, 2) applies the exactly same procedures in  
285 Eq. 43 and applies assumption B.7 (independent client).

## 286 **D.7 Bound the Gradient $\nabla f(w_0^t, \mathbf{w}^t)$**

287 Start with Eq. 52:

$$\begin{aligned} & \mathbb{E} (M^{t+1} - M^t) \\ & \leq -\frac{1}{4} \min \{ \eta_0, p_m \eta_m \} \mathbb{E} \|\nabla f(w_0^t, \mathbf{w}^t)\|^2 + Q_1 + Q_2 \end{aligned} \quad (54)$$

288 Summing over the global iteration  $t = 0, 1, \dots, T-1$ , arrange the equation and divided it by  $T$  from  
289 both sides.

$$\frac{1}{4T} \min \{ \eta_0, p_m \eta_m \} \sum_{t=0}^{T-1} \mathbb{E} \|\nabla f(w_0^t, \mathbf{w}^t)\|^2$$



$$\begin{aligned}
&\leq \frac{\mathbb{E}(M^0 - M^T)}{T} + Q_1 + Q_2 \\
&\stackrel{1)}{\leq} \frac{\mathbb{E}(f^0 - f^*)}{T} + Q_1 + Q_2
\end{aligned} \tag{55}$$

290 where 1)  $\mathbb{E}(M^0 - M^T) = f(w_0^0, \mathbf{w}^0) - f(w_0^T, \mathbf{w}^T) - \sum_{i=1}^{\tau} \theta_i \|\mathbf{w}^{T-i} - \mathbf{w}^{T-i}\|^2 \leq$   
291  $f(w_0^0, \mathbf{w}^0) - f(w_0^T, \mathbf{w}^T) \leq f^0 - f^*$ , we use  $f^0$  to denote  $f(w_0^0, \mathbf{w}^0)$  and applying assumption B.1.

292 Dividing  $\zeta = \frac{1}{4} \min\{\eta_0, p_m \eta_m\}$  from both sides:

$$\begin{aligned}
&\frac{1}{T} \sum_{t=0}^{T-1} \mathbb{E} \|\nabla f(w_0^t, \mathbf{w}^t)\|^2 \\
&\leq \frac{\mathbb{E}(f^0 - f^*)}{T\zeta} + \frac{Q_1}{\zeta} + \frac{Q_2}{\zeta} \\
&\leq \frac{\mathbb{E}(f^0 - f^*)}{T\zeta} \\
&\quad + \frac{1}{\zeta} \left( \eta_0 H_0^2 + 2L\eta_0^2 H_0^2 + 4 \sum_{m=1}^M p_m \eta_m \mathbf{G}_m^2 H_m^2 \right) \varepsilon + \left( 4 \sum_{m=1}^M p_m \eta_m \mathbf{G}_m^2 + L \sum_{m=1}^M p_m \eta_m^2 \mathbf{G}_m^2 \right) \Gamma \\
&\quad + \frac{1}{4\zeta} \sum_{m=1}^M p_m \eta_m \mu_m^2 L_m^2 d_{h_m}^2 \mathbf{G}_m^2 + \frac{2}{\zeta} \sum_{m=1}^M p_m L \eta_m^2 d_{h_m} \mathbf{G}_0^2 \mathbf{G}_m^2 + \frac{1}{2\zeta} \sum_{m=1}^M p_m L \eta_m^2 \mu_m^2 L_m^2 d_{h_m}^2 \mathbf{G}_m^2 \\
&\quad + \frac{1}{\zeta} L \eta_0^2 \sigma_0^2 \\
&\quad + \frac{\tau}{\zeta} \left( \eta_0 L_0^2 + 2L\eta_0^2 L_0^2 + 2 \sum_{m=1}^M p_m \eta_m L_m^2 \right) \left( 2 \sum_{m=1}^M p_m \eta_m^2 d_{h_m} \mathbf{G}_0^2 \mathbf{G}_m^2 \right. \\
&\quad \quad \quad \left. + \frac{1}{2} \sum_{m=1}^M p_m \eta_m^2 \mu_m^2 L_m^2 d_{h_m}^2 \mathbf{G}_m^2 + \sum_{m=1}^M p_m \eta_m^2 \mathbf{G}_m^2 \Gamma \right)
\end{aligned} \tag{56}$$

293 where 1) plugging in  $Q_1$ .

294 To simplify the result, let  $L_* = \max_m \{L, L_0, L_m\}$ ,  $\eta_0 = \eta_m = \eta \leq \frac{1}{4L_*}$ ,  $\frac{1}{p_*} = \min_m p_m$ ,  
295  $\mu_* = \max_m \{\mu_m\}$ ,  $d_* = \max_m \{d_{h_m}\}$ ,  $\mathbf{G}_* = \max_m \{\mathbf{G}_0, \mathbf{G}_m\}$ ,  $H_* = \max_m \{H_0, H_m\}$ , then  
296  $\zeta = \frac{1}{4} \min\{\eta_0, p_m \eta_m\} = \frac{\eta}{4p_*}$ . Eq. 56 can be further simplified:

$$\begin{aligned}
&\frac{1}{T} \sum_{t=0}^{T-1} \mathbb{E} \|\nabla f(w_0^t, \mathbf{w}^t)\|^2 \\
&\stackrel{1)}{\leq} \frac{4p_* \mathbb{E}(f^0 - f^*)}{T\eta} \\
&\quad + 4p_* \left( H_*^2 + 2L\eta H_*^2 + 4 \sum_{m=1}^M p_m \mathbf{G}_*^2 H_m^2 \right) \varepsilon + 4p_* \left( 4 \sum_{m=1}^M p_m \mathbf{G}_*^2 + L \sum_{m=1}^M p_m \eta \mathbf{G}_*^2 \right) \Gamma \\
&\quad + p_* \sum_{m=1}^M p_m \mu_*^2 L_*^2 d_*^2 \mathbf{G}_*^2 + 8p_* \sum_{m=1}^M p_m L \eta d_* \mathbf{G}_*^4 + 2p_* \sum_{m=1}^M p_m L \eta \mu_*^2 L_*^2 d_*^2 \mathbf{G}_*^2 \\
&\quad + 4p_* L \eta \sigma_0^2 \\
&\quad + 4p_* \tau \left( L_*^2 + 2L\eta L_*^2 + 2 \sum_{m=1}^M p_m L_m^2 \right) \left( 2 \sum_{m=1}^M p_m \eta^2 d_* \mathbf{G}_*^4 + \frac{1}{2} \sum_{m=1}^M p_m \eta^2 \mu_*^2 L_*^2 d_*^2 \mathbf{G}_*^2 + \sum_{m=1}^M p_m \eta^2 \mathbf{G}_*^2 \Gamma \right) \\
&\stackrel{2)}{\leq} \frac{4p_* \mathbb{E}(f^0 - f^*)}{T\eta}
\end{aligned}$$

$$\begin{aligned}
& + 4p_* (H_*^2 + 2L\eta H_*^2 + 4\mathbf{G}_*^2 H_*^2) \mathcal{E} + 4p_* (4\mathbf{G}_*^2 + L\eta \mathbf{G}_*^2) \Gamma \\
& + p_* \mu_*^2 L_*^2 d_*^2 \mathbf{G}_*^2 + 8p_* L\eta d_* \mathbf{G}_*^4 + 2p_* L\eta \mu_*^2 L_*^2 d_*^2 \mathbf{G}_*^2 \\
& + 4p_* L\eta \sigma_0^2 \\
& + 4p_* \tau (L_*^2 + 2L\eta L_*^2 + 2L_*^2) \left( 2\eta^2 d_* \mathbf{G}_*^4 + \frac{1}{2} \eta^2 \mu_*^2 L_*^2 d_*^2 \mathbf{G}_*^2 + \eta^2 \mathbf{G}_*^2 \Gamma \right) \\
& \stackrel{3)}{\leq} \frac{4p_* \mathbb{E} (f^0 - f^*)}{T\eta} \\
& + p_* (6H_*^2 + 16\mathbf{G}_*^2 H_*^2) \mathcal{E} + 17p_* \mathbf{G}_*^2 \Gamma \\
& + p_* \mu_*^2 L_*^2 d_*^2 \mathbf{G}_*^2 + 8p_* L\eta d_* \mathbf{G}_*^4 + 2p_* \eta \mu_*^2 L_*^3 d_*^2 \mathbf{G}_*^2 \\
& + 4p_* L\eta \sigma_0^2 \\
& + 28p_* \tau \eta^2 d_* \mathbf{G}_*^4 + 7p_* \tau \eta^2 \mu_*^2 L_*^4 d_*^2 \mathbf{G}_*^2 + 14p_* \tau L_*^2 \eta^2 \mathbf{G}_*^2 \Gamma \\
& \stackrel{4)}{\leq} \frac{4p_* \mathbb{E} (f^0 - f^*)}{T\eta} \\
& + \eta (8p_* L d_* \mathbf{G}_*^4 + 2p_* \mu_*^2 L_*^3 d_*^2 \mathbf{G}_*^2 + 4p_* L \sigma_0^2) \\
& + \eta^2 (28p_* \tau d_* \mathbf{G}_*^4 + 7p_* \tau \mu_*^2 L_*^4 d_*^2 \mathbf{G}_*^2 + 14p_* \tau L_*^2 \mathbf{G}_*^2 \Gamma) \\
& + \mu_*^2 (p_* L_*^2 d_*^2 \mathbf{G}_*^2) \\
& + \mathcal{E} (6p_* H_*^2 + 16p_* \mathbf{G}_*^2 H_*^2) \\
& + \Gamma (17p_* \mathbf{G}_*^2)
\end{aligned} \tag{57}$$

297 where 1) plugs in the above variables  $L_*, \eta, p_*, \zeta, \mu_*$ , 2) applies  $\sum_{m=1}^M p_m = 1$ , 3) simplify by  
298  $\eta \leq \frac{1}{4L_*}$ , 4) collect  $\eta, \mu_*, \mathcal{E}$

299 Suppose we set  $\eta = \frac{1}{\sqrt{T}}$ ,  $\mu_* = \frac{1}{\sqrt{T}}$ , and design the compression to make  $\mathcal{E} = \mathcal{O}\left(\frac{1}{\sqrt{T}}\right)$  and  
300  $\Gamma = \mathcal{O}\left(\frac{1}{\sqrt{T}}\right)^2$  the above equation becomes

$$\begin{aligned}
& \frac{1}{T} \sum_{t=0}^{T-1} \mathbb{E} \|\nabla f(w_0^t, \mathbf{w}^t)\|^2 \\
& \leq \frac{1}{\sqrt{T}} (4p_* \mathbb{E} (f^0 - f^*) + 8p_* L d_* \mathbf{G}_*^4 + 4p_* L \sigma_0^2 + 6p_* H_*^2 + 16p_* \mathbf{G}_*^2 H_*^2 + 17p_* \mathbf{G}_*^2) \\
& + \frac{1}{T} (28p_* \tau d_* \mathbf{G}_*^4 + p_* L_*^2 d_*^2 \mathbf{G}_*^2) \\
& + \frac{1}{T^{\frac{3}{2}}} (2p_* L_*^3 d_*^2 \mathbf{G}_*^2 + 14p_* \tau L_*^2 \mathbf{G}_*^2) \\
& + \frac{1}{T^2} (7p_* \tau \mu_*^2 L_*^4 d_*^2 \mathbf{G}_*^2)
\end{aligned} \tag{58}$$

301 Therefore,

$$\frac{1}{T} \sum_{t=0}^{T-1} \mathbb{E} \|\nabla f(w_0^t, \mathbf{w}^t)\|^2 = \mathcal{O}\left(\frac{d_h}{\sqrt{T}}\right) \tag{59}$$

302 where  $d_h = d_* = \max_m \{d_{h_m}\}$  (for clear notation),  $T$  is the number of communication rounds.

303 The proof of Theorem 5.2 is complete.  $\blacksquare$

---

<sup>2</sup>Refer to C-VFL [4] about how to design the compression to achieve the compression errors of  $\mathcal{O}\left(\frac{1}{\sqrt{T}}\right)$ .

## 304 E Experiment Details and Extra Experiments

### 305 E.1 Experiment Details

306 **Experiment Hardware and Software** The experiments were conducted on a Linux server with  
307 Intel(R) Xeon(R) Silver 4114 CPU @ 2.20GHz and the experiment is run on one Nvidia Tesla P100  
308 graphic card. PyTorch was used as the deep learning framework. We re-implement the framework  
309 by ourselves because all of the frameworks [18, 4, 5, 21] we compared were not open-source,  
310 and re-implementing the code helped make a fair comparison which eliminated the differences in  
311 implementation details of various methods.

312 **Feature Splitting Details** Regarding the dist-MNIST experiment in Section 6, we flattened the  
313 image and then equally distributed the dimensions among each client. Specifically, the first client  
314 received the upper half of each image, while the second client was allocated the lower half.

315 Regarding the dist-CIFAR-10 experiment in Section 6 (and section E.3 in this Appendix), we split the  
316 image by the last dimension. Therefore, the first client was assigned the left half, while the second  
317 client received the right half of each image.

### 318 Syn-ZOO-VFL

---

**Algorithm 1** The Synchronous Modification of ZOO-VFL [21]

---

```
0: Initialize variables for workers  $m \in [M]$ 
1: for  $t = 0, \dots, T - 1$  do
2:   Random sample a sample  $i$  (or batch  $B$ ).
3:   for client  $m$  in  $[M]$  in parallel do
4:     Client  $m$  compute and send  $h_{m,i} = h_m(w_m; x_{m,i})$  and  $\hat{h}_{m,i} = h_m(w_m + \mu \mathbf{u}_{m,i}; x_{m,i})$  to
       the server.
5:     The server calculates  $\delta_m = f_i(w_0, \dots, \hat{h}_{m,i} \dots) - f_i(w_0, h_{1,i}, \dots, h_{M,i})$  and send back to the
       client.
6:     Client  $m$  calculate the stochastic gradient w.r.t. its local parameter  $w_m$  with the  $\delta_m$  received
       from the server:  $\hat{\nabla}_{w_m} f_i(\cdot) = \frac{\phi(d_m)}{\mu} \delta_m \mathbf{u}_{m,i}$ 
7:     Client  $m$  update its parameter with gradient descent  $w_m \leftarrow w_m - \eta_m \hat{\nabla}_{w_m} f_i(\cdot)$ 
8:   end for
9:   The server calculates its local stochastic gradient estimation via  $\hat{\nabla}_{w_0} f_i(\cdot) =$ 
        $\frac{\phi(d_0)}{\mu} \left[ f_i(w_0 + \mu \mathbf{u}_{0,i}, \dots, \hat{h}_{m,i} \dots) - f_i(w_0, h_{1,i}, \dots, h_{M,i}; y_i) \right] \mathbf{u}_{0,i}$ 
10:  The server update its local parameter with gradient descent  $w_0 \leftarrow w_0 - \eta_0 \hat{\nabla}_{w_0} f_i(\cdot)$ 
11: end for
```

---

### 319 E.2 Computation Cost on Extra Propagation on the Server

320 Our method has extra computation cost on the server compared with other methods, however, the  
321 difference is negligible given the powerful computation performance of the server.

322 We repeat the experiment on dist-MNIST with the default setting (2 clients). To make the result more  
323 obvious, we **disable the GPU** to conduct this experiment, and we record the computational time as an  
324 index of the computational cost. We assume that the network latency is the same for all frameworks,  
325 and ignoring other minor operations in the implementation. The major factor which influences the  
326 computation cost is the propagation through the network.

327 The table below shows a comparison of the computation cost between different frameworks. Letter  
328 "F" means forward propagation, "B" means backward propagation, and the numeral preceding the  
329 letter indicates the number of propagations, for all frameworks, we only count the propagation time.

Table 2: Computational Cost for Extra Propagation

Framework	Client	Server	Client Comp. Time per Epoch (s)	Server Comp. per Epoch (s)
Split learning [18]	F+B	F+B	0.86	0.90
Syn-ZOO-VFL	2F	3F	0.64	1.00
Compressed-VFL [4]	F+B	F+B	0.86	0.89
VAFL [5]	2F	F+B	1.10	1.52
ZOO-VFL [21]	2F	3F	0.92	1.49
VAFL[5]+DP[3]	F+B	F+B	1.10	1.52
Ours	F+B	101F+B	1.15	49.02

330 **E.3 Dist-CIFAR-10 Experiments**

331 **E.3.1 Comparing with SOTA Frameworks**

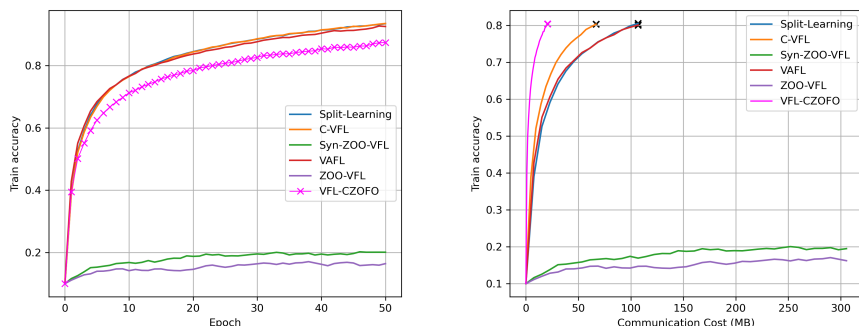
332 Following the training procedure outlined in section 6, we utilized the optimal configuration across all  
 333 frameworks. Table 3 presents a summary of the test accuracy and communication metrics at various  
 334 stages of convergence. Our achieved test accuracy is comparable to the SOTA VFL methodology.  
 335 Furthermore, our communication costs are significantly lower than those reported by the leading  
 336 VFL communication efficiency research. In contrast, the pure ZOO-based VFL is unable to attain  
 337 convergence to a practical model due to the large dimensionality of the model for optimization.

Table 3: Test Accuracy and Evaluation of the Total Communication Cost.

	Privacy Security	Test Accuracy	Cost (80%)	Cost (total)
Split learning [18]	✗	84.31 ± 0.28	107 MB	381 MB
Compressed-VFL [4]	✗	84.10 ± 0.18	67 MB	240 MB
VAFL [5]	✗	83.16 ± 0.03	184 MB	400 MB
Syn-ZOO-VFL	✓	18.08 ± 0.33	-	-
ZOO-VFL [21]	✓	17.96 ± 0.92	-	-
Ours	✓	82.82 ± 0.29	21 MB	45 MB

338 (-) represents that the model cannot converge to a usable model after the entire training process.

339 Figure 2 illustrates a plot of the training accuracy against epoch (Figure 2-a) and communication  
 340 cost (Figure 2-b). As depicted in (a), our framework exhibits a convergence rate comparable to  
 341 that of other frameworks. Specifically, regarding the communication cost, as indicated in (b), our  
 342 communication cost is significantly lower than that of other communication-efficient algorithms.



(a) Dist-CIFAR-10 by epochs

(b) Dist-CIFAR-10 by comm. cost

Figure 2: Comparing with other VFL Framework on Dist-CIFAR10

343 The cross means that the training accuracy reaches 80%.

### 344 E.3.2 Dist-CIFAR-10 Ablation Study

345 **Ablation Study on Zeroth Order Optimization** Figure 3 performs an ablation study on the  
 346 application of ZOO on the connection layer. We implemented the Avg-RandGradEst using various  
 347 sampling times  $q$ . The results indicate that exclusively applying ZOO yields communication costs  
 348 comparable to those of FOO-based VFL in each communication budget.

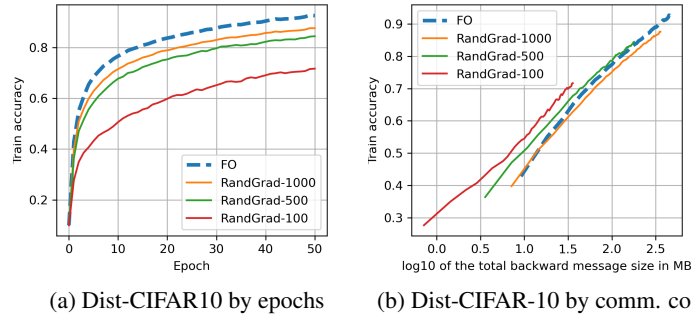


Figure 3: Ablation Study on ZO with Dist-CIFAR-10

349 Table 4 presents the test accuracy of the method and the total backward cost of implementing ZOO  
 350 on the output layer. The table shows that the application of ZOO decreases the total communica-  
 351 tion required for the entire training process. With all the sampling times  $q$  provided in the table,  
 352 communication costs are reduced with a slight utility trade-off.

Table 4: Ablation Study on ZO with Dist-CIFAR-10

ZO Type	Test Accuracy	Backward Cost
FO	$83.16 \pm 0.03$	200 MB
RandGradEst-1000	$82.10 \pm 0.28$	156 MB
RandGradEst-500	$81.28 \pm 0.17$	78 MB
RandGradEst-100	$72.83 \pm 0.20$	16 MB

353 **Ablation Study on Compression** Figure 4 displays the results of the ablation study on communi-  
 354 cation for both forward and backward messages. The plot represents the training accuracy against the  
 355 communication cost. The results indicate that the utilization of a certain degree of compression (8, 4,  
 356 2 bits) led to a reduction in communication costs without significantly affecting the convergence of  
 357 the model.

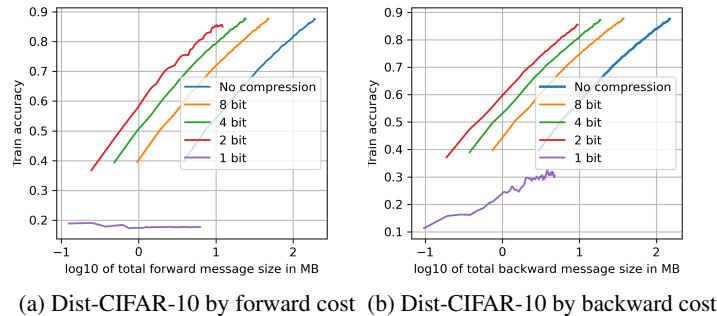


Figure 4: Ablation Study on Compression with Dist-CIFAR-10

358 Table 5 presents the test accuracy and total communication cost for compression on forward and  
 359 backward messages. The results suggest that compressing to a certain degree does not significantly  
 360 impact test accuracy, but it considerably reduces the communication cost. Therefore, we may  
 361 implement compression to a certain level, such as 4 bits for both the forward and backward messages.

Table 5: Ablation Study on Compression with Dist-CIFAR-10

Compression	Test Accuracy	Forward/Backward Cost
No Compression	$82.10 \pm 0.28$	200 MB
Forward-8 bit	$81.90 \pm 0.24$	50 MB
Forward-4 bit	$82.64 \pm 0.29$	25 MB
Forward-2 bit	$81.55 \pm 0.23$	13 MB
Forward-1 bit	$17.68 \pm 0.70$	6 MB
Backward-8 bit	$82.03 \pm 0.25$	39 MB
Backward-4 bit	$82.31 \pm 0.30$	20 MB
Backward-2 bit	$81.15 \pm 0.34$	10 MB
Backward-1 bit	$31.03 \pm 0.67$	5 MB

#### 362 E.4 Experiments on GiveMeSomeCredit Dataset

363 To simulate a real-world VFL scenario, we utilize the GiveMeSomeCredit dataset [2]. This dataset  
 364 comprises 15,000 samples, each consisting of a single label and 10 features. The first client was  
 365 assigned the first 5 features for each sample, while the second client received the remaining 5 features.  
 366 Given the dataset’s significant class imbalance, we address this issue by downsampling the majority  
 367 (negative) class to achieve an equal size with the positive class. Subsequently, we divide the dataset  
 368 into a 75% training set and a 25% testing set. we employ a straightforward linear model ( $y = Wx$ ) on  
 369 the client side. This model takes the local features of the client as input and generates two predictions:  
 370 one for the positive class and another for the negative class. We set the batch size to 64 during training,  
 371 and the model undergoes 100 epochs. The learning rate is chosen as 0.01 from the option of [0.1,  
 372 0.01, 0.001]. Additionally, we select the value of  $\mu$  as 0.001 from the options [0.1, 0.001, 0.0001,  
 373 0.00001] through preliminary experiments. We set the sampling time  $q = 10$  for our framework.  
 374 The experiment results for different methods’ test accuracy and the communication cost is shown in  
 375 table 6. As demonstrated in the table our method significantly reduces the communication cost of  
 376 training.

Table 6: Test Accuracy and Evaluation of the Total Communication Cost.

	Test Accuracy	Cost (70%)	Cost (total)
Split learning [18]	$72.18 \pm 0.01$	5.7 MB	38.3 MB
Compressed-VFL [4]	$72.13 \pm 0.03$	3.8 MB	24.1 MB
VAFL [5]	$72.26 \pm 0.29$	5.4 MB	38.3 MB
Syn-ZOO-VFL	$71.74 \pm 0.53$	9.2 MB	38.3 MB
ZOO-VFL [21]	$71.85 \pm 0.70$	4.6 MB	38.6 MB
Ours	$72.76 \pm 0.29$	0.7 MB	5.8 MB

377 Figure 5 displays the corresponding convergence of all the frameworks, The figure shows that while  
 378 all the frameworks converge similarly, our approach notably reduces the communication cost for each  
 379 epoch.

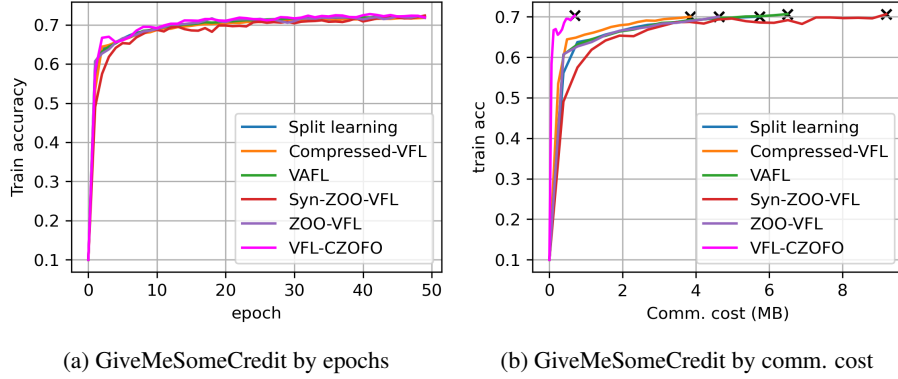


Figure 5: Comparing with other VFL Framework on GiveMeSomeCredit Task

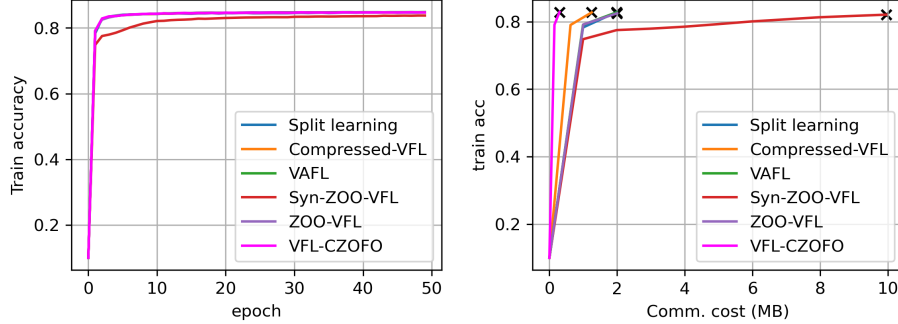
### 380 E.5 Experiments on a9a Dataset

381 The a9a dataset [20, 1] encompasses a total of 32,561 training samples and 16,281 testing samples.  
 382 Each sample has one label and 123 features. In our experiment, the first client was assigned the first  
 383 62 features of each sample, while the second client received the remaining 61 features. Our approach  
 384 employs a linear model similar to the one presented in section E.4. Specifically, client 1’s model has  
 385 an input size of 62, whereas client 2’s model has an input size of 61. Both models have an output  
 386 size of 2. The training procedure is the same as the experiment in section E.4. We set the batch  
 387 size to 64 during training, and the model is trained 100 epochs. The learning rate is chosen as 0.01.  
 388 Additionally, we select the value of  $\mu$  as 0.001. We set the sampling time  $q = 10$  for our framework.  
 389 The experiment results for different methods’ test accuracy and the communication cost is shown in  
 390 table 7. As demonstrated in the table our method significantly reduces the communication cost of  
 391 training.

Table 7: Test Accuracy and Evaluation of the Total Communication Cost.

	Test Accuracy	Cost (82%)	Cost (total)
Split learning [18]	$84.84 \pm 0.01$	2.0 MB	99.4 MB
Compressed-VFL [4]	$84.85 \pm 0.02$	1.2 MB	62.5 MB
VAFL [5]	$85.08 \pm 0.01$	2.0 MB	99.4 MB
Syn-ZOO-VFL	$84.55 \pm 0.05$	10.0 MB	99.6 MB
ZOO-VFL [21]	$84.84 \pm 0.01$	2.0 MB	100.1 MB
Ours	$84.86 \pm 0.01$	0.3 MB	14.9 MB

392 Figure 6 displays the corresponding convergence of all the frameworks, The figure shows that while  
 393 all the frameworks converge almost identically (with the exception of Syn-ZOO-VFL, whose lines do  
 394 not overlap), our approach notably reduces the communication cost for each epoch.



(a) a9a by epochs (b) a9a by comm. cost  
 Figure 6: Comparing with other VFL Framework on a9a Dataset

### 395 E.6 Experiment on the Privacy-utility Trade-off

396 In the experiments in section 6.2 and section 6.3, we only demonstrated a typical trade-off of our  
 397 framework. However, our framework also has the capability to achieve the same test accuracy as  
 398 Split-Learning, compressed-VFL, and VAFL, applying a corresponding privacy-utility trade-off.  
 399 Note that these three baselines sacrifice privacy and get higher test accuracy (“test-accuracy-focused  
 400 trade-off”), while the last three baselines (VAFL+DP, Syn-ZOO-VFL, ZOO-VFL) take a balance  
 401 between privacy and utility (“balanced trade-off”).

402 To achieve the test-accuracy-focused trade-off, we use the coordinate-wise gradient estimator (Coord-  
 403 GradEst) to separately estimate the partial for each dimension[14, 11]:

$$\hat{\nabla}_{h_{m,i}} f_i(w_0, h_{1,i}, \dots, h_{M,i}) = \frac{1}{2\mu_m} \sum_{l=1}^{d_{h_m}} \underbrace{[f_i(h_{m,i} + \mu_m e_m^l) - f_i(h_{m,i} - \mu_m e_m^l)]}_{\delta_{m,i}^l} e_m^l$$

404 where  $e_m^l \in \mathcal{R}^{d_{h_m}}$  is a  $d_{h_m}$ -dimensional standard bias vector with 1 at its  $l$ -th dimension, and 0s  
 405 otherwise. To apply the coordinate-wise estimation, the server sends  $\{\delta_{m,i}^l\}_{l=1}^{d_{h_m}}$  back to the client. It  
 406 is noteworthy that the backward message  $\{\delta_{m,i}^l\}_{l=1}^{d_{h_m}}$  has the same size as  $\frac{\partial f_i}{\partial h_{m,i}}$ . Both are vectors  
 407 of decimal numbers with dimensions of  $d_{h_m}$ . Therefore, if neither method uses compression, the  
 408 communication cost for VAFL-CZOFO (CoordGradEst) is identical to that of VAFL.

409 Besides, regarding the "balanced trade-off", the basic zeroth-order estimator (ZOE) we used in  
 410 section 6 has a large forward bias. To improve this, we applied a slightly “advanced” centralized  
 411 version of ZOE so that we reached higher test accuracy and better convergence:

$$\hat{\nabla}_{h_{m,i}} f_i(w_0, h_{1,i}, \dots, h_{M,i}) = \frac{\phi(d_{h_m})}{q\mu_m} \sum_{j=1}^q \underbrace{[f_i(h_{m,i} + \mu_m u_{m,i}^j) - f_i(h_{m,i} - \mu_m u_{m,i}^j)]}_{\delta_{m,i}^j} u_{m,i}^j$$

412 With this centralized ZOE, we can achieve a smoother convergence and a similar privacy budget.

413 Table 8 illustrates our method’s capacity to achieve diverse privacy-utility trade-offs when compared  
 414 to the baselines. In each scenario, our framework successfully achieves the specified privacy budget  
 415 while maintaining a test accuracy similar to that of the baselines.

Table 8: Privacy-utility Trade-off of VFL-CZOFO

	Privacy	Trade-off type	Test Accuracy
VAFL	✗	Test-accuracy-focused trade-off	97.36 ± 0.14
VFL-CZOFO (CoordGradEst)	✗	Test-accuracy-focused trade-off	97.35 ± 0.05
VAFL + DP	$\epsilon = 95$	Balanced trade-off	95.94 ± 0.29
VFL-CZOFO (Avg-RandGradEST)	$\epsilon = 95$	Balanced trade-off	96.32 ± 0.22



416 **E.7 Experiments on More Clients**

417 In section 6 of the paper, we only consider a typical scenario with only two clients. Therefore, we  
 418 conducted experiments with four and eight clients to further assess the performance of our framework  
 419 on a larger scale.

420 The dataset splitting setting of the experiments follows the dist-MNIST experiment. For the experiment  
 421 involving four clients in section, the first client received the uppermost 1/4 of each image; the second  
 422 client obtained the segment spanning from the upper 1/4 to 1/2; the third client from the lower 1/2 to  
 423 3/4; finally, the fourth client was assigned the bottommost 1/4. A similar split was implemented for  
 424 the experiment involving eight clients.

425 The models deployed on each client are identical to the one presented in Section 6. Similarly, the  
 426 server model is described in detail in Section 6. However, it is worth noting that with the number of  
 427 clients changed, the input size of the first layer of the server has been adjusted to  $4 \times 64 = 256$  for  
 428 the 4-client experiments and  $8 \times 64 = 512$  for the 8-client experiments.

429 **E.7.1 Training Efficiency and Communication Cost**

430 We conducted the same experiment on training efficiency and communication cost as in section 6.3.  
 431 The outcomes for four clients are depicted in Figure 7 and detailed in Table 9. Similarly, the outcomes  
 432 for eight clients are presented in Figure 8 and detailed in Table 10. These results collectively  
 433 substantiate the efficacy of our method in diminishing communication costs, particularly within  
 434 scenarios involving a higher number of clients.

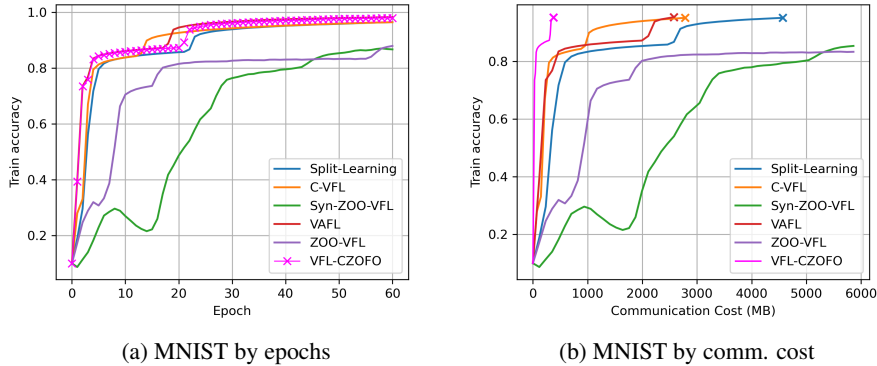


Figure 7: Training Efficiency and Communication Cost Experiment on 4 Clients

Table 9: Test Accuracy and Comm. Cost (4 Clients)

	Privacy	Test Accuracy	Cost (95%)	Cost (total)
Split learning	✗	$97.67 \pm 0.03$	4570 MB	11718 MB
Compressed-VFL	✗	$97.78 \pm 0.12$	2783 MB	7325 MB
VAFL	✗	$97.60 \pm 0.07$	2703 MB	12288 MB
VAFL+DP	✓	$96.72 \pm 0.21$	3179 MB	12288 MB
Syn-ZOO-VFL	✓	$83.97 \pm 0.51$	-	11722 MB
ZOO-VFL	✓	$87.42 \pm 0.25$	-	12291 MB
Ours	✓	$96.60 \pm 0.08$	537 MB	1579 MB

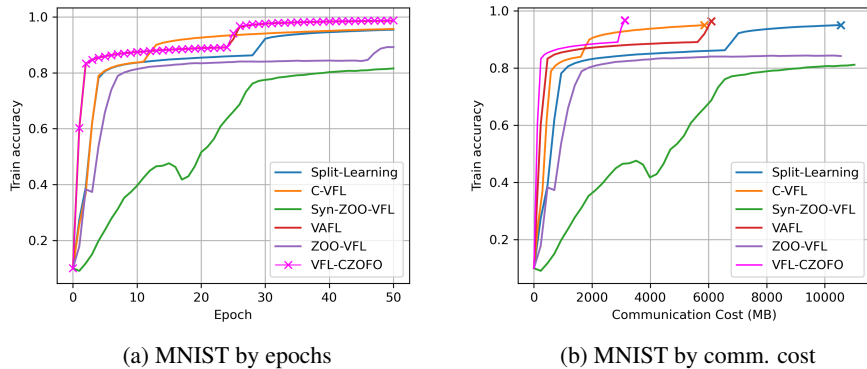


Figure 8: Training Efficiency and Communication Cost Experiment on 8 Clients

Table 10: Test Accuracy and Comm. Cost (8 Clients)

	Privacy	Test Accuracy	Cost (95%)	Cost (total)
Split learning	✗	97.46 ± 0.08	10547 MB	23438 MB
Compressed-VFL	✗	97.51 ± 0.09	5860 MB	14649 MB
VAFL	✗	97.41 ± 0.04	6390 MB	24579 MB
VAFL+DP	✓	96.62 ± 0.17	8132 MB	24579 MB
Syn-ZOO-VFL	✓	82.64 ± 0.57	-	23443 MB
ZOO-VFL	✓	89.49 ± 0.38	-	24093 MB
Ours	✓	96.81 ± 0.12	3272 MB	12590 MB

### 435 E.7.2 The Computational Cost

436 With more clients, the server may take more computational costs on the server. Therefore, we also  
 437 conducted an experiment on the computational cost of the server and the clients. The setting of this  
 438 experiment follows the experiment in section E.2 but changes the number of clients to four and eight.  
 439 The result is shown in Table 11.

Table 11: Computational Cost for Propagation (More Clients)

The number of Clients	Clients' Comp. Time per Epoch (s)	Server's Comp. Time per Epoch (s)
2	1.15	49.02
4	2.65	122.20
8	9.81	384.29

### 440 References

- 441 [1] a9a dataset. <https://archive.ics.uci.edu/ml/datasets/Adult>. Accessed: 2023-5-10.
- 442 [2] GiveMeSomeCredit dataset. <https://www.kaggle.com/c/GiveMeSomeCredit>. Accessed: 2023-5-10.
- 443 [3] Martin Abadi, Andy Chu, Ian Goodfellow, H Brendan McMahan, Ilya Mironov, Kunal Talwar, and  
 444 Li Zhang. Deep learning with differential privacy. In *Proceedings of the 2016 ACM SIGSAC conference on*  
 445 *computer and communications security*, pages 308–318, 2016.
- 446 [4] Timothy J Castiglia, Anirban Das, Shiqiang Wang, and Stacy Patterson. Compressed-vfl: Communication-  
 447 efficient learning with vertically partitioned data. In *International Conference on Machine Learning*, pages  
 448 2738–2766. PMLR, 2022.
- 449 [5] Tianyi Chen, Xiao Jin, Yuejiao Sun, and Wotao Yin. Vaf: a method of vertical asynchronous federated  
 450 learning. *arXiv preprint arXiv:2007.06081*, 2020.

- 451 [6] Cynthia Dwork, Aaron Roth, et al. The algorithmic foundations of differential privacy. *Foundations and*  
452 *Trends® in Theoretical Computer Science*, 9(3–4):211–407, 2014.
- 453 [7] Matt Fredrikson, Somesh Jha, and Thomas Ristenpart. Model inversion attacks that exploit confidence  
454 information and basic countermeasures. In *Proceedings of the 22nd ACM SIGSAC conference on computer*  
455 *and communications security*, pages 1322–1333, 2015.
- 456 [8] Chong Fu, Xuhong Zhang, Shouling Ji, Jinyin Chen, Jingzheng Wu, Shanqing Guo, Jun Zhou, Alex X  
457 Liu, and Ting Wang. Label inference attacks against vertical federated learning. In *31st USENIX Security*  
458 *Symposium (USENIX Security 22)*, Boston, MA, 2022.
- 459 [9] Xiang Gao, Bo Jiang, and Shuzhong Zhang. On the information-adaptive variants of the admm: an iteration  
460 complexity perspective. *Journal of Scientific Computing*, 76(1):327–363, 2018.
- 461 [10] Saeed Ghadimi and Guanghui Lan. Stochastic first-and zeroth-order methods for nonconvex stochastic  
462 programming. *SIAM Journal on Optimization*, 23(4):2341–2368, 2013.
- 463 [11] Bin Gu, Zhouyuan Huo, and Heng Huang. Zeroth-order asynchronous doubly stochastic algorithm with  
464 variance reduction. *arXiv preprint arXiv:1612.01425*, 2016.
- 465 [12] Bin Gu, An Xu, Zhouyuan Huo, Cheng Deng, and Heng Huang. Privacy-preserving asynchronous vertical  
466 federated learning algorithms for multiparty collaborative learning. *IEEE transactions on neural networks*  
467 *and learning systems*, 2021.
- 468 [13] Xiao Jin, Pin-Yu Chen, Chia-Yi Hsu, Chia-Mu Yu, and Tianyi Chen. Cafe: Catastrophic data leakage in  
469 vertical federated learning. *Advances in Neural Information Processing Systems*, 34:994–1006, 2021.
- 470 [14] Sijia Liu, Bhavya Kailkhura, Pin-Yu Chen, Paishun Ting, Shiyu Chang, and Lisa Amini. Zeroth-order  
471 stochastic variance reduction for nonconvex optimization. *Advances in Neural Information Processing*  
472 *Systems*, 31, 2018.
- 473 [15] Yang Liu, Yan Kang, Liping Li, Xinwei Zhang, Yong Cheng, Tianjian Chen, Mingyi Hong, and Qiang  
474 Yang. A communication efficient vertical federated learning framework. *Scanning Electron Microscop Meet*  
475 *at*, 2019.
- 476 [16] Xinjian Luo, Yuncheng Wu, Xiaokui Xiao, and Beng Chin Ooi. Feature inference attack on model  
477 predictions in vertical federated learning. In *2021 IEEE 37th International Conference on Data Engineering*  
478 *(ICDE)*, pages 181–192. IEEE, 2021.
- 479 [17] Jiankai Sun, Xin Yang, Yuanshun Yao, and Chong Wang. Label leakage and protection from forward  
480 embedding in vertical federated learning. *arXiv preprint arXiv:2203.01451*, 2022.
- 481 [18] Praneeth Vepakomma, Otkrist Gupta, Tristan Swedish, and Ramesh Raskar. Split learning for health:  
482 Distributed deep learning without sharing raw patient data. *arXiv preprint arXiv:1812.00564*, 2018.
- 483 [19] Haiqin Weng, Juntao Zhang, Feng Xue, Tao Wei, Shouling Ji, and Zhiyuan Zong. Privacy leakage of  
484 real-world vertical federated learning. *arXiv preprint arXiv:2011.09290*, 2020.
- 485 [20] Zhi-Qiang Zeng, Hong-Bin Yu, Hua-Rong Xu, Yan-Qi Xie, and Ji Gao. Fast training support vector  
486 machines using parallel sequential minimal optimization. In *2008 3rd international conference on*  
487 *intelligent system and knowledge engineering*, volume 1, pages 997–1001. IEEE, 2008.
- 488 [21] Qingsong Zhang, Bin Gu, Zhiyuan Dang, Cheng Deng, and Heng Huang. Desirable companion for  
489 vertical federated learning: New zeroth-order gradient based algorithm. In *Proceedings of the 30th ACM*  
490 *International Conference on Information & Knowledge Management*, pages 2598–2607, 2021.
- 491 [22] Qingsong Zhang, Bin Gu, Cheng Deng, and Heng Huang. Secure bilevel asynchronous vertical federated  
492 learning with backward updating. In *Proceedings of the AAAI Conference on Artificial Intelligence*,  
493 volume 35, pages 10896–10904, 2021.
- 494 [23] Bo Zhao, Konda Reddy Mopuri, and Hakan Bilen. idlg: Improved deep leakage from gradients. *arXiv*  
495 *preprint arXiv:2001.02610*, 2020.
- 496 [24] Ligeng Zhu, Zhijian Liu, and Song Han. Deep leakage from gradients. *Advances in neural information*  
497 *processing systems*, 32, 2019.